On the eNB-Based Energy Saving Cooperation Techniques for LTE Access Networks

Md. Farhad Hossain, Kumudu S. Munasinghe and Abbas Jamalipour

School of Electrical and Information Engineering, The University of Sydney, NSW 2006, Australia

{md.hossain, kumudu.munasinghe, abbas.jamalipour}@sydney.edu.au

Abstract

Energy efficiency is one of the top priorities for future cellular networks, which could be accomplished by implementing cooperative mechanisms. In this paper, we propose three eNB-centric energy saving cooperation techniques for LTE systems. These techniques named as intra-network, inter-network and joint cooperation, involve traffic-aware intelligent cooperation among eNBs belong to the same or different networks. Our proposed techniques dynamically reconfigure LTE access networks in real-time utilizing less number of active eNBs and save energy. In addition, these techniques are distributed and self-organizing in nature. Analytical models for evaluating switching dynamics of eNBs under these cooperation mechanisms are also formulated. We thoroughly investigate the proposed system under different number of cooperating networks, traffic scenarios, eNB power profiles and their switching thresholds. Optimal energy savings while maintaining QoS is also evaluated. Results indicate a significant reduction in network energy consumption. System performance in terms of network capacity utilization, switching statistics, additional transmit power and eNB sleeping patterns is also investigated. Finally, a comprehensive comparison with other works is provided for further validation.

Index Terms

Energy efficiency; cooperative cellular networks; self-organizing networks; LTE networks

I. Introduction

Unprecedented growth in the number of users and applications is pushing energy consumption in wireless networks at an exceptional rate. This remarkable rise in energy utilization is exerting tremendous detrimental impact on both the economical and the environmental aspects. In a cellular network, the most significant part of energy expenditure goes for radio access network (RAN) equipment amounting 60%-90% of its total consumption [1], [2], [3]. Therefore, reduction of energy consumption in RANs can significantly supplement the energy efficiency of cellular networks. On the other hand, self-organizing networks (SONs) with autonomous operation, control and maintenance can manage networks with minimal human effort and reduced complexity [4], [5], [6]. Therefore,

most recently, designing of self-organizing type energy efficient cellular access networks have drawn paramount attention among researchers.

In this paper, we propose and explore the potential of evolved node B (eNB) centric three different cooperation techniques for improving the energy efficiency of long term evolution (LTE) evolved universal terrestrial radio access networks (E-UTRANs). Proposed techniques are named as intra-network cooperation, inter-network cooperation and joint cooperation. Intra-network cooperation involves cooperation among eNBs belong to the same E-UTRAN, while the cooperation among eNBs belong to different E-UTRANs are employed in the inter-network cooperation. Finally, in joint cooperation, former two techniques are combinely utilized for further increasing the energy savings. These techniques are implemented at each eNB and require no human assistance. Therefore, they are distributed and self-organizing in nature.

Using these cooperation mechanisms, based on the instantaneous traffic in eNBs, E-UTRANs are reconfigured in real-time using fewer eNBs and the redundant eNBs are switched to sleep mode for saving energy. At the same time, quality of service (QoS) constraints, namely, call blocking and network coverage are maintained. For accomplishing the purpose, eNBs cooperatively exchange information, redistribute traffic, adjust their transmission range and switch operating modes. Also, unlike many other proposals, eNBs in our system do not require any prior knowledge of their traffic generation patterns and thus, compliant with the dynamically fluctuating traffic scenarios. Traffic dynamics observed both in time and space of real networks have been exploited for reconfiguring E-UTRANs. System performance has been investigated through extensive simulations over a wide range of network scenarios, which identifies significant reduction in network energy consumption. Impact of different network parameters, namely, switching thresholds, traffic distributions, network traffic level and power consumption profiles of eNBs on the savings are also presented.

Our main contributions in this proposed research can be summarized as follows:

• We propose and outline the details of three energy saving distributed and self-organizing type cooperation techniques, while maintaining satisfactory service level. Necessary algorithms are also presented in detail.

• Comprehensive simulations are carried out for evaluating the system performance in terms of energy savings, network capacity utilization, switching statistics, additional transmit power, sleeping patterns, etc.

• Analytical models for evaluating the sleeping probability of eNBs as a function of the system parameters are formulated for all the three cooperation techniques. Analytical results closely resembles with the simulation results, which firmly validates our simulation models.

• Exhaustive search technique is then used for evaluating the optimal energy savings. Correspond-

ing network behaviour is then further explored.

• We also compare our techniques with the other recently published works, which further validates our proposal.

The rest of the paper is organized as follows. Related works are summarized in Section II. Section III presents the detail system model and algorithms, while system parameters are outlined in Section IV. Section V formulates the analytical models. In Section VI, we provide the results with thorough discussion, followed by the conclusion in Section VII.

II. Related Works

Over the last few years, various schemes for energy efficient cellular access networks have been published [7]. These schemes can be broadly categorized as, turning on/off base transceiver stations (BTSs) of a single network [3], [5], [8], [9], [10], [11]; cell zooming [12]; dimming of BTSs [13]; use of smaller and heterogeneous cell sizes [14], [15], [16]; coordinated multi-point transmission (CoMP) [17]; and cooperative sharing of BTSs belong to multiple networks [18], [19], [20], [21]. Without specifying any implementation mechanism, switching-off lightly loaded eNBs for energy conservation is included as a use-case in LTE [5]. Manual and predefined switching schemes for turning off BTSs during low traffic time were proposed in [8], [9], which are not compatible with SONs. In contrast, the schemes presented in [10] and [11] utilized dynamic shutting down of BTSs, however, reactivation of them is again manual. Whereas, authors in [3] presented some greedy algorithms and formed cost optimization problems for theoretically evaluating energy savings by switching on and off BTSs.

On the other hand, a preliminary study of a quite different approach termed as cell zooming was proposed in [12]. In this approach, depending on the traffic level, BTSs shrink or expand their transmit range and even can switch to sleep mode for saving energy. Alternately, [13] proposed dimming services and frequencies of BTSs. However, due to random request generation for services by users, blackout of services for any duration always has a possibility of call request failures. Furthermore, potential energy savings from deployment of smaller and heterogeneous cell sizes along with the switching off BTSs was presented in [14], [15]; while [16] reported that effective energy savings may not be realizable by deploying small cells. In [17], the issue of energy savings in cellular networks was approached by focusing on the network planning stage. In this paper, inter-cell cooperation is used to achieve CoMP transmission and consequently, a new network can be deployed using less number of BTSs. On the other hand, sharing BTSs among multiple network operators is an alternate option for reducing network energy consumption. In our previous work, we presented a simulation based analysis of this kind [18]. However, the system model is very basic and

no QoS constraint is considered as well. Besides, initial studies using simplified system models for identifying the potential of energy savings from cooperative sharing of BTSs were also presented in [19], [20], [21].

Although several schemes have been proposed for energy efficiency of RANs, research in this field is still in its infancy. Previous proposed schemes have their own limitations, such as, use of simplified system model and inadequate analysis, not being of fully autonomous, requirement of knowledge on traffic patterns, etc. This has motivated us to carry out this proposed research.

III. System Model and Algorithms

Due to the random call making and mobility pattern of users, cellular network traffic generation exhibits both temporal and spatial variation [22], [23]. Regardless, current networks are over provisioned to meet the worst case scenario. For instance, expecting peak-traffic scenario when all the cell sites would be required to support the users, all the sites are always left in active mode, even during very low traffic period. However, contemporary macro cells consume nearly equal power irrespective of carried traffic [24], [25], [26]. Thus, during low traffic times, while fewer sites can meet the user demand, a substantial amount of energy can be saved by switching some cell sites into sleep mode. This paper particularly focuses on this concept.

In this section, we outline three different cooperative frameworks for E-UTRANs employing different cooperation mechanisms, named as, intra-network cooperation, inter-network cooperation and joint cooperation (i.e., a combination of the previous two). These mechanisms, employing mutual cooperation among eNBs, reconfigure E-UTRANs by regulating the number of active and sleep mode eNBs in a self-organizing fashion, while maintaining QoS and thus, energy savings is achieved. In active mode, an eNB has the full functionality as of conventional eNBs. Exchange of necessary information among eNBs and formulation of necessary decisions for the proposed cooperation are also carried out in active mode. On the other hand, a sleep mode eNB neither carries any user traffic nor formulates any decision. However, it listens to any wake-up request from other eNBs for switching to active mode.

Once the decision of switching to sleep mode is made for an eNB, no new connection is allowed and after the hand-over of all the ongoing connections to the other eNB(s), this eNB switches to sleep mode. On the other hand, a sleep mode eNB immediately switches to active mode after the reception of wake-up request from any eNB. Switching time from active to sleep mode must be sufficient to allow users to hand-over. At the same time, switching should be fast, otherwise it might offset the benefits of energy savings. In contrast, the smaller the switching time from sleep mode

to active mode, the better will be the system performance. For a realistic cellular network, typical switching time is estimated in the order of 30 seconds [27].

Here, we consider a system model of N co-located LTE networks serving a geographical area. Complete system model is shown in Fig. 1, which is explained in detail in the following sections. The notations used here below in the algorithm section are summarized in Table I. On the other hand, general assumptions used in system modeling can be summarized as follows: (a) eNBs are capable to switch between active and sleep modes. (b) eNBs belongs to the same E-UTRAN communicates through X2 interface. While, the S4 interface of LTE core network is used for exchanging information among different E-UTRANs via serving gateways (SGWs). (c) Energy requirement for signaling among eNBs is negligible. (d) Perfect power control is implemented in both the uplink and the downlink such that data rates of the swapped users remain unchanged. (e) Mobile stations (MSs) have multi-mode interfaces for supporting all the cooperating E-UTRANs.

A. Intra-network Cooperation

1) Methodology: In intra-network cooperation, an eNB intelligently cooperates with its neighboring eNBs belong to the same E-UTRAN, while the neighboring eNBs also cooperate with their neighboring eNBs and so on. Under this cooperation, based on the instantaneous traffic, eNBs dynamically exchange information, swap traffic, adjust transmit power and switch operating modes. Thus, each network is reconfigured using fewer number of active eNBs and energy savings is achieved. Each eNB is equally responsible for collecting information; coordinating with neighbors; and devising and implementing decisions. To carry out these functions, no operator assistance is required for eNBs, which makes the scheme self-organizing in nature.

Referring to the i^{th} ranked E-UTRAN in Fig. 1, we can explain the technique in detail. For instance, eNB $\mathcal{B}_{i,7}$ can switch from active to sleep mode if there are candidate sets of neighboring eNBs with sufficient idle capacity for supporting its traffic. Based on the location of an eNB and the cell layout, number of candidate sets varies. For example, $[\mathcal{B}_{i,1}, \mathcal{B}_{i,4}]$, $[\mathcal{B}_{i,2}, \mathcal{B}_{i,5}]$, and $[\mathcal{B}_{i,3}, \mathcal{B}_{i,6}]$ are three such candidate sets for $\mathcal{B}_{i,7}$. Traffic of $\mathcal{B}_{i,7}$ is distributed to the best candidate set, which can support all of its users and keep call blocking within target limit. An eNB sharing the traffic of other eNB(s) is named as acceptor eNB. Here, $\mathcal{B}_{i,1}$ and $\mathcal{B}_{i,4}$ are acceptors for $\mathcal{B}_{i,7}$.

An acceptor eNB needs to increase its transmit power in certain directions for covering the sleep mode eNBs. For facilitating this power adjustment, eNBs are assumed to be equipped with multiple sets of power controlled directional antenna(s), one set for one neighboring eNB. For example, an eNB requires up to six, four and two sets of antennas in hexagonal, rectangular and linear layouts respectively. A single power amplifier and a single spectrum pool are shared among these antennas.

Multiple input multiple output (MIMO) technology can also be implemented by equipping each of these sets with multiple antennas (e.g., 2 antennas/set for 2x2 MIMO).

2) Algorithm: In the proposed algorithm, based on own instantaneous traffic load, eNBs initiate their traffic distribution process. Instantaneous traffic load $\mathcal{L}_{i,j}(t)$ of $\mathcal{B}_{i,j}$ is defined as the number of LTE physical resource blocks (PRBs) in use at time t. Switching thresholds of $\mathcal{B}_{i,j}$, denoted by a vector $\Psi_{i,j} = \left(\vartheta_{i,j}, \omega_{i,j}, \varepsilon_{i,j}\right)$, are used for instigating this traffic distribution. Thus, distribution of $\mathcal{L}_{i,j}(t)$ is triggered if either, (a) $\mathcal{L}_{i,j}(t) < \vartheta_{i,j}$, or (b) $\mathcal{L}_{i,j}(t) \geq \omega_{i,j}$. However, when $\mathcal{B}_{i,j}$ is an acceptor, it can accept traffic from neighbors as long as its total traffic is less than $\varepsilon_{i,j}$.

We here summarize the information required for traffic distribution of $\mathcal{B}_{i,j}$: $s_{i,j} \in \{0, 1\}$, $p_{i,j}$, $\mathbf{U}_{i,j} = \left\{u_{i,j}^{(1)}, u_{i,j}^{(2)}, ..., u_{i,j}^{(W_{i,j})}\right\}$ and $\mathbf{V}_{i,j} = \left\{v_{i,j}^{(1)}, v_{i,j}^{(2)}, ..., v_{i,j}^{(Z_{i,j})}\right\}$. Here, if $\mathcal{B}_{i,j}$ is in active mode, $s_{i,j} = 1$, otherwise $s_{i,j} = 0$ (i.e., sleep mode). While, $\mathbf{U}_{i,j}$ is the set of acceptor eNBs for $\mathcal{B}_{i,j}$, $\mathbf{V}_{i,j}$ the set of eNBs for whom $\mathcal{B}_{i,j}$ is an acceptor and $0 \leq W_{i,j}, Z_{i,j} \leq N_{\mathcal{B}_{i,j}}$. Other required information includes the ID, traffic load and operating mode vectors of neighboring eNBs denoted by $\mathcal{I}_{i,j} = \left[\mathcal{B}_{i,j}^{(1)}, \mathcal{B}_{i,j}^{(2)}, ..., \mathcal{B}_{i,j}^{(N_{\mathcal{B}_{i,j}})}\right]$, $\mathcal{A}_{i,j} = \left[\mathcal{L}_{i,j}^{(1)}, \mathcal{L}_{i,j}^{(2)}, ..., \mathcal{L}_{i,j}^{(N_{\mathcal{B}_{i,j}})}\right]$ and $\mathcal{S}_{i,j} = \left[s_{i,j}^{(1)}, s_{i,j}^{(2)}, ..., s_{i,j}^{(N_{\mathcal{B}_{i,j}})}\right]$ respectively. From the received ID vector $\mathcal{I}_{i,j}$, $\mathcal{B}_{i,j}$ generates a $M_{i,j} \times P$ matrix $\mathbb{C}_{i,j} = \left[\mathbf{C}_{i,j}^{(1)}; \mathbf{C}_{i,j}^{(2)}; ...; \mathbf{C}_{i,j}^{(M_{i,j})}\right]$ in which each row is a candidate set for $\mathcal{B}_{i,j}$, where $\mathbf{C}_{i,j}^{(m)} = \left[C_{i,j}^{m,1}, C_{i,j}^{m,2}, ..., C_{i,j}^{m,P}\right]$. $\mathbb{C}_{i,j}$ is then divided into two sub-matrices: $q_{i,j} \times P$ matrix $\mathbb{C}_{i,j}^{a}$ and $r_{i,j} \times P$ matrix $\mathbb{C}_{i,j}^{s}$, such that, $q_{i,j} + r_{i,j} = M_{i,j}$. Here, $\mathbb{C}_{i,j}^{a} = \left[\mathbf{F}_{i,j}^{(1)}; \mathbf{F}_{i,j}^{(2)}; ...; \mathbf{F}_{i,j}^{(q_{i,j})}\right]$ and all eNBs in $\mathbf{F}_{i,j}^{(s)} = \left[F_{i,j}^{s,1}, F_{i,j}^{s,2}, ..., F_{i,j}^{s,P}\right]$ are in active mode. Whereas, $\mathbb{C}_{i,j}^{s} = \left[\mathbf{H}_{i,j}^{(1)}; \mathbf{H}_{i,j}^{(2)}; ..., \mathbf{H}_{i,j}^{(r_{i,j})}\right]$, where at least one eNB in $\mathbf{H}_{i,j}^{(t)} = \left[H_{i,j}^{t,1}, H_{i,j}^{t,2}, ..., H_{i,j}^{t,P}\right]$ is in sleep mode.

Now, for case (a) (i.e., low traffic in $\mathcal{B}_{i,j}$), traffic is distributed only to the active eNBs. Therefore, during $\mathcal{L}_{i,j}(t) < \vartheta_{i,j}$, the best set of eNBs for traffic distribution is selected only from $\mathbb{C}_{i,j}^{a}$. In contrast, for $\mathcal{L}_{i,j}(t) \geq \omega_{i,j}$, which refers a heavy traffic in $\mathcal{B}_{i,j}$, $\mathcal{L}_{i,j}(t)$ can be distributed to both the lightly loaded active mode and zero traffic sleep mode eNBs. That means, the best set is evaluated either from $\mathbb{C}_{i,j}^{a}$ or $\mathbb{C}_{i,j}^{s}$ with a higher preference of $\mathbb{C}_{i,j}^{a}$. However, for this case, we propose four alternative options (presented in Table III) for selecting eNBs to distribute $\mathcal{L}_{i,j}(t)$, which are sequentially attempted. The four options are, (i) full traffic distribution to $\mathbb{C}_{i,j}^{a}$, (ii) partial traffic distribution to $\mathbb{C}_{i,j}^{a}$, (iii) full traffic distribution to $\mathbb{C}_{i,j}^{s}$, and (iv) partial traffic distribution to $\mathbb{C}_{i,j}^{s}$. Proposed sequence ensures the higher preference of distributing traffic to the active eNBs than to the sleeping eNBs. Thus, it is guaranteed that sleep mode eNBs are not switched to active mode unless it is absolutely necessary for maintaining call blocking within target limit. This in turn reduces the number of switching in eNBs and increases energy savings.

Algorithms for intra-network cooperation are presented in pseudo code form in Table II and III. Let, $\mathbf{F}_{i,j}^{*}$ and $\mathbf{H}_{i,j}^{*}$ be the best sets from $\mathbb{C}_{i,j}^{a}$ and $\mathbb{C}_{i,j}^{s}$ respectively. Pseudo code of the selection process

of $\mathbf{F}^*_{i,j}$ for $\mathcal{B}_{i,j}$ used in Table II (i.e., when $\mathcal{L}_{i,j}(t) < \vartheta_{i,j}$) is presented in Table IV. Similar procedure is used for finding out $\mathbf{F}^*_{i,j}$ and $\mathbf{H}^*_{i,j}$ used in Table III.

B. Inter-network Cooperation

1) Methodology: Nowadays, almost any city around the world is being served by more than one cellular mobile operator [19], [21]. Therefore, in this section, we extend our focus on exploiting the availability of multiple networks through inter-network cooperation. As shown in Fig. 1, geographically co-located N E-UTRANs mutually cooperate for saving energy. For the simplicity, we assume that the co-located eNBs are of equal size. At a particular location, based on the instantaneous total traffic load of the N co-located eNBs, one from each cooperating E-UTRAN, the traffic is redistributed among the N eNBs. Thus, some of these N eNBs can switch to sleep mode and reduce the overall energy consumption. Sufficient number of eNBs is left active for supporting the total load of this location. Again, similar to the intra-network cooperation, no operator assistance is required. Traffic load can be redistributed according to an agreed policy among the network operators, such as, a pre-defined ranking of the networks or a dynamic ranking derived from the instantaneous traffic scenario. In this paper, we have adopted the pre-defined ranking policy. Without losing the generality, the ranking of the E-UTRANs in descending order is taken as $1, 2, ..., N$. The algorithm for traffic distribution is discussed below.

2) Algorithm: Let us denote, $\mathbb{D}_{i,j} = \left\{\mathcal{B}^{(k)}_{i,j} : k = 1, 2, ..., N, k \neq i\right\}$, $\mathcal{A}_{i,j} = \left\{\mathcal{L}^{(k)}_{i,j} : k = 1, 2, ..., N, k \neq i\right\}$, $\mathcal{S}_{i,j} = \left\{s^{(k)}_{i,j} : k = 1, 2, ..., N, k \neq i\right\}$ and $\mathcal{P}_{i,j} = \left\{p^{(k)}_{i,j} : k = 1, 2, ..., N, k \neq i\right\}$ as the ID, traffic load, operating mode and transmit power sets of the candidate eNBs for $\mathcal{B}_{i,j}$ respectively. Then, based on the ranking of networks and the operating mode of candidate eNBs, $\mathbb{D}_{i,j}$ is divided into four mutually exclusive sets: $\mathbb{D}^{L,a}_{i,j} = \left\{\mathcal{B}^{(k)}_{i,j} : k > i, s^{(k)}_{i,j} = 1\right\}$, $\mathbb{D}^{L,s}_{i,j} = \left\{\mathcal{B}^{(k)}_{i,j} : k > i, s^{(k)}_{i,j} = 0\right\}$, $\mathbb{D}^{H,a}_{i,j} = \left\{\mathcal{B}^{(k)}_{i,j} : k < i, s^{(k)}_{i,j} = 1\right\}$, and $\mathbb{D}^{H,s}_{i,j} = \left\{\mathcal{B}^{(k)}_{i,j} : k < i, s^{(k)}_{i,j} = 0\right\}$. Here, the superscripts 'L', 'H', 'a' and 's' stand for 'Lower ranked', 'Higher ranked', 'Active mode' and 'Sleep mode' respectively.

Similar to the intra-network cooperation, the two cases, a) $\mathcal{L}_{i,j} < \vartheta_{i,j}$, and b) $\mathcal{L}_{i,j} \geq \omega_{i,j}$ are dealt in different ways. In case of (a), $\mathcal{B}_{i,j}$ can distribute traffic only to the lower ranked active eNBs, i.e., to eNBs in $\mathbb{D}^{L,a}_{i,j}$. However, for (b), following the order denoted by $\mathbb{S} = \left(\mathbb{D}^{L,a}_{i,j} \Rightarrow \mathbb{D}^{H,a}_{i,j} \Rightarrow \mathbb{D}^{L,s}_{i,j} \Rightarrow \mathbb{D}^{H,s}_{i,j}\right)$, $\mathcal{B}_{i,j}$ can distribute traffic to all the four sets. This proposed sequence preserves the network ranking as well as the higher preference of selecting active eNBs over the sleep mode eNBs for distributing traffic. During the traffic distribution to a particular set, $\mathcal{B}_{i,j}$ distributes sequentially to eNBs of that set starting from the lowest ranked one. As an instance, load distribution by i^{th} ranked network is shown at the bottom part of Fig. 1. Pseudo code of the traffic distribution algorithms are presented in Table V and VI.

C. Joint Cooperation

1) Methodology: Under joint cooperation, intra-network cooperation and inter-network cooperation are jointly applied for achieving higher level of energy savings. At each instance of execution of the cooperation mechanisms, both the cooperation techniques are carried out one after another. Either of the two techniques can be carried out first followed by the other.

2) Algorithm: In this paper, in the first phase, intra-network cooperation is carried out inside each network, which reconfigures respective networks with the reduced number of active eNBs. Then, in the second phase, inter-network cooperation among the networks are carried out for further reducing the number of active eNBs. The algorithm is presented in Table VII.

IV. System Parameters

In this section, we present the performance metrics, such as, sleeping probabilities of eNBs, number of switching, net energy savings, network capacity utilization, etc. Furthermore, an optimization approach for evaluating the optimal savings is presented here.

A. Probability of Sleeping of eNBs

As defined before, $s_{i,j}(t) \in \{0, 1\}$ is the operating mode of $\mathcal{B}_{i,j}$ at time t. Therefore, the average sleeping probability of an eNB in the proposed network over time T can be given by,

$$P_S = \left[\frac{1}{NN_iT} \sum_{i=1}^{N} \sum_{j=1}^{N_i} \int_0^T \left\{ 1 - s_{i,j}(t) \right\} dt \right] \times 100\% \tag{1}$$

B. Number of Switching

Let n_s be the total number of instances over time T at which the algorithms are executed. Then, the average number of instances in percentage at which switching occurs can be given by,

$$\mathcal{N}_{Sw} = \frac{1}{NN_in_s} \sum_{i=1}^{N} \sum_{j=1}^{N_i} \left[\sum_{k=1}^{n_s} XOR\left(s_{i,j}(k), s_{i,j}(k-1) \right) \right] \times 100\%, s_{i,j}(k) = 1 \text{ for } k \leq 0, \forall i, \forall j \tag{2}$$

C. Power Consumption Profiles of eNBs

Total power consumption and the achievable energy savings from a network may largely depend on the power consumption profiles of eNBs. For quantitative evaluation of the impact of power models, we have used a generalized power consumption model for $\mathcal{B}_{i,j}$ [3],

$$P_{i,j}^T(t) = \left(1 - \delta_{i,j}\right) \overline{\mathcal{L}}_{i,j}(t) P_{i,j}^{Op} + \delta_{i,j} P_{i,j}^{Op} \tag{3}$$

where, $0 \leq \overline{\mathcal{L}}_{i,j}(t) \leq 1.0$, $P^{T}_{i,j}(t)$ and $P^{Op}_{i,j}$ are the instantaneous load factor, instantaneous operating power and maximum operating power of fully utilized $\mathcal{B}_{i,j}$ respectively. Whereas, $0 \leq \delta_{i,j} \leq 1$ is a constant. Thus, we can define three kinds of eNBs - constant energy consumption (CEC) model $\left(\delta_{i,j} = 1\right)$, fully energy proportional (FEP) model $\left(\delta_{i,j} = 0\right)$, and non-energy proportional (NEP) model $\left(0 < \delta_{i,j} < 1\right)$. On the other hand, $P^{Op}_{i,j} = g_{i,j}P^{Tx}_{i,j} + h_{i,j}$, where, $P^{Tx}_{i,j}$ is the maximum transmit power; and $g_{i,j}$ and $h_{i,j}$ are constants for $\mathcal{B}_{i,j}$ [26], [28]. Here, $g_{i,j}$ performs the dimensioning of $P^{Op}_{i,j}$ with $P^{Tx}_{i,j}$ and $h_{i,j}$ models the fraction of $P^{Op}_{i,j}$, which remains constant irrespective of $P^{Tx}_{i,j}$.

D. Transmit Power Adjustment in eNBs

For estimating the required transmit power for each eNB, we have used link budget analysis. Required transmit power of user k in $\mathcal{B}_{i,j}$ for maintaining required signal-to-interference-noise-ratio ($\text{SINR}^{(k)}$) is equal to $10^{0.1\left[\text{SINR}^{(k)}(dB) - P^{(k)}_{G}(dB) + P^{(k)}_{L}(dB)\right]}$ watts. Here, $P^{(k)}_{G}$ is the sum of all gains from an eNB to an MS, such as, antenna gains, MIMO gains, eNB cyclic combining gain and so on. Whereas, $P^{(k)}_{L}$ represents the combined effect of all the deteriorating factors, such as, path loss, interference, eNB and MS noise figure, fading margin, feeder loss, etc. Thus, for each eNB, we can evaluate the instantaneous total transmit power $\mathscr{P}^{Tx}_{i,j}(t)$ and the additional transmit power $\mathscr{P}^{Tx\bigstar}_{i,j}(t)$ required for serving all the active users in $\mathcal{B}_{i,j}$ at time t.

Extended coverage with additional transmit power may change the inter-cell interference level at different areas of the proposed network. A wide range of techniques for managing inter-cell interference in OFDMA based cellular networks, such as, frequency reuse schemes (e.g., integer frequency, fractional frequency and soft frequency reuse) [29], [30]; partial isolation technique [31]; cancellation, coordination and randomization [32]; etc. are available in the literature. They can be easily adopted in our system. Therefore, in this paper, we have not explicitly considered interference issue and left it for our future works.

E. Energy Savings

Let, $E^{AON}_{i,j}$ and $E^{SON}_{i,j}$ be the total energy consumption in $\mathcal{B}_{i,j}$ while being used in a conventional network (i.e., always active) and the proposed network respectively. Thus,

$$E^{AON}_{i,j} = \int_{0}^{T} P^{T}_{i,j}(t)dt \quad \text{and} \quad E^{SON}_{i,j} = \int_{0}^{T} \left[s_{i,j}(t)P^{T\bigstar}_{i,j}(t) + \left(1 - s_{i,j}(t)\right)P^{Sleep}_{i,j}\right]dt, \ \forall i, \forall j \qquad (4)$$

In (4), $P^{T\bigstar}_{i,j}(t) = P^{T}_{i,j}(t)$ is calculated from (3) by replacing $P^{Tx}_{i,j}$ with $\left[P^{Tx}_{i,j} + \mathscr{P}^{Tx\bigstar}_{i,j}(t)\right]$. Also, $P^{Sleep}_{i,j}$ is the sleep mode power requirement of $\mathcal{B}_{i,j}$. Again, since switching of eNBs from active to sleep mode and vice versa takes some time, we need to consider the energy consumed during the switching

times. Total switching time in $\mathcal{B}_{i,j}$ is, $t_{i,j}^{Sw} = S_{\mathcal{B}_{i,j}}^{AS}\left(t_{Sw}^{AS} + \tau_{i,j} t_B^{AS}\right) + S_{\mathcal{B}_{i,j}}^{SA} t_{Sw}^{SA}$ and total energy consumption during this time is, $E_{i,j}^{Sw} = \int_0^{t_{i,j}^{Sw}} P_{i,j}^{T\bigstar}(t)dt$. Here, t_{Sw}^{AS} and t_{Sw}^{SA} are the switching times from active to sleep mode and vice versa, $S_{\mathcal{B}_{i,j}}^{AS}$ and $S_{\mathcal{B}_{i,j}}^{SA}$ are the number of switching from active to sleep mode and vice versa, t_B^{AS} is the waiting time of $\mathcal{B}_{i,j}$ before starting to switch to sleep mode, and $0 \leq \tau_{i,j} \leq 1$ is the fraction of $S_{\mathcal{B}_{i,j}}^{AS}$ at which $\mathcal{B}_{i,j}$ has to wait. Therefore, average net energy savings per eNB can be given by,

$$E_{Sav} = \frac{1}{NN_i} \sum_{i=1}^{N} \sum_{j=1}^{N_i} \left[\frac{E_{i,j}^{AON} - E_{i,j}^{SON} - E_{i,j}^{Sw}}{E_{i,j}^{AON}} \right] \times 100\% \tag{5}$$

F. Optimal Energy Savings and Design Parameters

Here, we define three optimization problems, which use exhaustive search technique for evaluating the maximum energy savings and the corresponding parameters. First optimization problem, denoted as P1, defines the optimal savings as the achievable maximum energy savings keeping call blocking probability $P_i^B, \forall i$ within a standard limit $(P_i^B)_{Th}$, while imposing no restrictions on the number of switching $\mathcal{N}_{Sw}$. The second optimization problem P2 maximizes energy savings as well as minimizes $\mathcal{N}_{Sw}$, while maintains call blocking within $(P_i^B)_{Th}$. The last optimization objective P3 evaluates the maximum energy savings keeping both $P_i^B, \forall i$ and $\mathcal{N}_{Sw}$ within their respective threshold limits. The optimization problems are presented below:

$$\text{(P1)} \arg\max_{\vartheta_{i,j}, \omega_{i,j}, \varepsilon_{i,j}} E_{Sav} \quad s.t., \quad P_i^B \leq (P_i^B)_{Th}, \forall i$$

$$\text{(P2)} \arg\max_{\vartheta_{i,j}, \omega_{i,j}, \varepsilon_{i,j}} E_{Sav} \quad s.t., \quad P_i^B \leq (P_i^B)_{Th}, \forall i \quad \min \mathcal{N}_{Sw}$$

$$\text{(P3)} \arg\max_{\vartheta_{i,j}, \omega_{i,j}, \varepsilon_{i,j}} E_{Sav} \quad s.t., \quad P_i^B \leq (P_i^B)_{Th}, \forall i \quad \mathcal{N}_{Sw} \leq \mathcal{N}_{Sw}^{Th}$$

Additional conditions for P1, P2, P3:

$$\omega_{i,j} \geq \vartheta_{i,j}, \varepsilon_{i,j} > \vartheta_{i,j}, \varepsilon_{i,j} > \omega_{i,j}, \forall i, \forall j$$

$$\vartheta_{i,j}, \omega_{i,j}, \varepsilon_{i,j} \geq 0, \forall i, \forall j$$

G. Network Capacity Utilization Improvement (NCUI)

Here, we define the parameter NCUI as below which quantifies the gain in network capacity utilization by our proposed system. First we define, capacity utilization efficiency (CUE) for a network as given by,

$$\text{CUE} = \frac{\sum_{i=1}^{N} \sum_{j=1}^{N_i} \int_0^{T_{i,j}} \left[\mathcal{L}_{i,j}(t) / R_{i,j} \right] dt}{\sum_{i=1}^{N} \sum_{j=1}^{N_i} T_{i,j}} \tag{6}$$

where, $R_{i,j}$ and $T_{i,j}$ are the total number of PRBs and total active time of $\mathcal{B}_{i,j}$ respectively. The higher the value of CUE, the more efficient a network is in utilizing its available capacity. Then we can write,

$$\text{NCUI} = \left[\frac{\text{CUE of the proposed network}}{\text{CUE of the original network}} - 1\right] \times 100\% \tag{7}$$

H. Call Generation Model

In traffic modeling, call arrival process is usually assumed time-homogeneous. However, due to the temporal variation in call generation, actual arrival process is time-inhomogeneous, where call generation intensity varies with time and space. We have modeled call generation by Poisson process, and considered both time-homogeneous and time-inhomogeneous cases. A time-inhomogeneous process is generated by multiplying a time-homogeneous process with a rate function $0 \leq f(t) \leq 1$. Two such rate functions used in this paper are shown in Fig. 2.

We assume that in $\mathcal{B}_{i,j}$, there are $U_{i,j}$ classes of services each of having constant call duration equal to $h_{i,j}^{(u)}$. Then, the instantaneous total traffic load of $\mathcal{B}_{i,j}$ at time t can be given by,

$$\mathcal{L}_{i,j}(t) = \alpha_{i,j} \sum_{u=1}^{U_{i,j}} \rho_{i,j}^{(u)} h_{i,j}^{(u)} \eta_{i,j}^{(u)} f_{i,j}^{(u)}(t), \forall i, \forall j \tag{8}$$

where, $\rho_{i,j}^{(u)}$ is a Poisson random variable with parameter $\lambda_{i,j}^{(u)}$; $f_{i,j}^{(u)}(t)$ is the rate function; and $\eta_{i,j}^{(u)}$ is the number of required channels (i.e., PRBs) for class u. Random variable $\alpha_{ij} \geq 0$ models the variation of peak load among eNBs.

I. Call Blocking Probability

Multi-dimensional Erlang-B formula has been used for evaluating the call blocking probability. A state of $\mathcal{B}_{i,j}$ can be given as, $\overline{\gamma}_{i,j} = \left(\gamma_{i,j}^{(1)}, \gamma_{i,j}^{(2)}, ..., \gamma_{i,j}^{(U_{i,j})}\right)$, where, $\gamma_{i,j}^{(u)}$ is the number of active calls of class u. We can also write, $\overline{\eta}_{i,j} = \left(\eta_{i,j}^{(1)}, \eta_{i,j}^{(2)}, ..., \eta_{i,j}^{(U_{i,j})}\right)$. Thus, the state space of $\mathcal{B}_{i,j}$ becomes, $\Omega_{i,j} = \left\{\gamma_{i,j} : \overline{\gamma}_{i,j}(\overline{\eta}_{i,j})^T \leq \Upsilon_{i,j}, \gamma_{i,j}^{(k)} \geq 0, \forall k\right\}$, where $\Upsilon_{i,j}$ is the total number of channels in $\mathcal{B}_{i,j}$. Let $\Omega_{i,j}^{(u)} = \left\{\gamma_{i,j} : \Upsilon_{i,j} - \overline{\gamma}_{i,j}(\overline{\eta}_{i,j})^T < \eta_{i,j}^{(u)}, \gamma_{i,j}^{(k)} \geq 0, \forall k\right\} \subseteq \Omega_{i,j}$ and $a_{i,j}^{(u)} = \lambda_{i,j}^{(u)} h_{i,j}^{(u)}$. Then, the call blocking probability of class u in $\mathcal{B}_{i,j}$ can be given by,

$$P_{i,j}^{u,B} = \frac{G\left(\Omega_{i,j}^{(u)}\right)}{G\left(\Omega_{i,j}\right)}, \text{ where, } G\left(\Omega_{i,j}\right) = \sum_{\gamma_{i,j} \in \Omega_{i,j}} \prod_{u=1}^{U_{i,j}} \frac{\left(a_{i,j}^{(u)}\right)^{\gamma_{i,j}^{(u)}}}{\gamma_{i,j}^{(u)}}, G\left(\Omega_{i,j}^{(u)}\right) = \sum_{\gamma_{i,j} \in \Omega_{i,j}^{(u)}} \prod_{u=1}^{U_{i,j}} \frac{\left(a_{i,j}^{(u)}\right)^{\gamma_{i,j}^{(u)}}}{\gamma_{i,j}^{(u)}} \tag{9}$$

Thus, average call blocking probability in i^{th} network, $P_i^B = \sum_{j=1}^{N_i} \sum_{u=1}^{U_{i,j}} \lambda_{i,j}^{(u)} P_{i,j}^{u,B} / \sum_{j=1}^{N_i} \sum_{u=1}^{U_{i,j}} \lambda_{i,j}^{(u)}$.

V. Analytical Models

In this section, we formulate the analytical models for evaluating the sleeping probabilities of eNBs under the proposed cooperation mechanisms.

A. Intra-network Cooperation

In intra-network cooperation, switching of operating mode of an eNB depends only on the current load in eNBs and their operating modes at the previous instance. Thus, this process can be modeled as a Markov process. State space of i^{th} E-UTRAN can be given by, $\mathbb{S}_i^{Intra} = \left\{(s_{i,1}, s_{i,2}, ..., s_{i,N_i}) : s_{i,j} \in \{0,1\}, j = 1, 2, ..., N_i \right\}$. Total number of states is equal to 2^{N_i}, which grows exponentially with N_i and thus becomes extremely cumbersome for solving using Markov chain. Therefore, in this paper, a heuristic approach has been used in developing the analytical model.

Recalling from Section III-A, $\mathbf{C}_{i,j}^{(m)} = \left[C_{i,j}^{m,1}, C_{i,j}^{m,2}, ..., C_{i,j}^{m,P}\right], \forall i, \forall j$ is the $m^{th}(m = 0, 1, ..., M_{i,j})$ candidate set for $\mathcal{B}_{i,j}$ and $C_{i,j}^{m,k}$ is the $k^{th}(k = 1, 2, ..., P)$ candidate eNB in $\mathbf{C}_{i,j}^{(m)}$.

Let us define the following independent events $\forall j, \forall m, \forall k$:
$E_{i,j}^{(m)} = \left\{\mathcal{B}_{i,j} \text{ distributes load to } \mathbf{C}_{i,j}^{(m)} \text{ and switches to sleep}\right\}$ and $A_{i,j}^{m,k} = \left\{C_{i,j}^{m,k} \text{ is in active mode}\right\}$.

Considering that at time t, $\mathcal{B}_{i,j}$ is not serving as acceptor for any of its candidate eNBs, the probability of occurring $E_{i,j}^{(n)}(n = 0, 1, 2, ..., M_{i,j})$ at time t can be expressed as below,

$$Pr\left\{E_{i,j}^{(n)}\right\} = \left[Pr\left\{\mathcal{L}_{i,j} < \vartheta_{i,j}\right\} \times \prod_{k=1}^{P} P^{\Delta}\left\{A_{i,j}^{n,k}\right\} + Pr\left\{\mathcal{L}_{i,j} \geq \omega_{i,j}\right\}\right] \times \prod_{k=1}^{P} Pr\left\{\varepsilon_{i,j}^{n,k} - \mathcal{L}_{i,j}^{n,k} > \beta_{i,j}^{n,k}\mathcal{L}_{i,j}\right\} \quad (10)$$

where, $\mathcal{L}_{i,j}^{n,k}$ and $\varepsilon_{i,j}^{n,k}$ are the load and acceptance threshold of $C_{i,j}^{n,k}$ respectively; $\beta_{i,j}^{n,k}$ is the fraction of $\mathcal{L}_{i,j}$ to be distributed to $C_{i,j}^{n,k}$ and $\sum_{k=1}^{P}\beta_{i,j}^{n,k} = 1$; $Pr\left\{E_{i,j}^{(0)}\right\} = 0$; $P^{\Delta}\left\{A_{i,j}^{n,k}\right\}$ is the $Pr\left\{C_{i,j}^{n,k} \text{ is active at time } (t - \Delta t)\right\}$ and equal to 0, $\forall t \leq 0, \forall i, \forall j, \forall n, \forall k$.

For convenience, we have omitted the time index here and will bring back later. As per our algorithm, if $\mathcal{B}_{i,j}$ is already serving as acceptor for any of the candidate eNBs of the other $(M_{i,j} - 1)$ candidate sets, $\mathbf{C}_{i,j}^{(m)}, m \neq n$, then $\mathcal{B}_{i,j}$ can't switch to sleep mode by simply distributing its current load to the n^{th} set. Considering this fact, (10) is modified as below.

$$Pr\left\{\overline{X_{i,j}^{(n)}}\right\} = \prod_{\substack{m=1 \\ m\neq n}}^{M_{i,j}} Pr\left\{\mathcal{B}_{i,j} \text{ is acceptor for none of the eNBs in } \mathbf{C}_{i,j}^{(m)}\right\} = \left[\prod_{\substack{k=1 \\ m=1, m\neq n}}^{P}\left[1 - F_{i,j}^{m,k}P^{\Delta}\left\{S_{i,j}^{m,k}\right\}\right]\right]$$
$$\times \left[\prod_{\substack{k=1 \\ m=2, m\neq n}}^{P}\left[1 - F_{i,j}^{m,k}P^{\Delta}\left\{S_{i,j}^{m,k}\right\}\right]\right] \times ... \times \left[\prod_{\substack{k=1 \\ m=M_{i,j}, m\neq n}}^{P}\left[1 - F_{i,j}^{m,k}P^{\Delta}\left\{S_{i,j}^{m,k}\right\}\right]\right] \quad (11)$$

Here, $P^{\Delta}\left\{S_{i,j}^{m,k}\right\} = 1 - P^{\Delta}\left\{A_{i,j}^{m,k}\right\}$; $F_{i,j}^{m,k} = 1/M_{i,j}^{m,k}$, if $M_{i,j}^{m,k} \neq 0$ and $F_{i,j}^{m,k} = 0$, if $M_{i,j}^{m,k} = 0$. Also, $M_{i,j}^{m,k}$ is the number of candidate sets for $C_{i,j}^{m,k}$.

Therefore, the modified $Pr\left\{E_{i,j}^{(n)}\right\}$ can be given as,

$$\widetilde{Pr}\left\{E_{i,j}^{(n)}\right\} = Pr\left\{E_{i,j}^{(n)}\right\} \times Pr\left\{\overline{X_{i,j}^{(n)}}\right\} \tag{12}$$

Since $\mathcal{B}_{i,j}$ can distribute load to one of its $M_{i,j}$ candidate sets, conditional probability of $\mathcal{B}_{i,j}$ conditioned on RV α (defined in Appendix) to switch to sleep mode at time t can be given by,

$$P_{i,j}^{S,Intra}|_{\alpha} = \widetilde{Pr}\left\{\bigcup_{n=0}^{M_{i,j}} E_{i,j}^{(n)}\right\} = 1 - \prod_{n=0}^{M_{i,j}}\left[1 - \widetilde{Pr}\left\{E_{i,j}^{(n)}\right\}\right] = 1 - \prod_{n=0}^{M_{i,j}}\left[1 - \left[\left\{1 - Q\left(\frac{\frac{\vartheta_{i,j}}{\alpha f_{i,j}(t)} - \mu_{x_{i,j}}}{\sqrt{\sigma_{x_{i,j}}^2}}\right)\right\}\right.\right.$$
$$\left.\left. \times \prod_{k=1}^{P} P^{\Delta}\left\{A_{i,j}^{n,k}\right\} + Q\left(\frac{\frac{\omega_{i,j}}{\alpha f_{i,j}(t)} - \mu_{x_{i,j}}}{\sqrt{\sigma_{x_{i,j}}^2}}\right)\right] \times \prod_{k=1}^{P}\left\{1 - Q\left(\frac{\varepsilon_{i,j} - \mu_{y_{i,j}}}{\sqrt{\sigma_{y_{i,j}}^2}}\right)\right\} \times Pr\left\{\overline{X_{i,j}^{(n)}}\right\}\right] \tag{13}$$

The derivation of the expressions used in (13) is presented in Appendix.

Assuming $\alpha \sim U[a, b]$, unconditional probability $P_{ij}^{S,Intra}$ at time t can be written as,

$$P_{i,j}^{S,Intra}(t) = \frac{1}{b-a}\int_{a}^{b} P_{i,j}^{S,Intra}|_{\alpha} d\alpha \tag{14}$$

Then, the probability that an eNB in i^{th} network sleeps at time t (also equal to the fraction of eNBs in sleep mode) becomes, $P_{i}^{S,Intra}(t) = \frac{1}{N_i}\sum_{j=1}^{N_i} P_{i,j}^{S,Intra}(t), \forall i$. Finally, averaging (14) for all eNBs as well as time t, average sleeping probability of an eNB in i^{th} network is given by,

$$P_{i,avg}^{S,Intra} = \left[\frac{1}{N_i T}\sum_{j=1}^{N_i}\int_{0}^{T} P_{i,j}^{S,Intra}(t)dt\right] \times 100\%, \forall i \tag{15}$$

B. Inter-network Cooperation

Similar to the intra-network cooperation, switching of operating modes of N eNBs at j^{th} location, one from each network is a Markov process. Here, the state space for j^{th} location is, $\mathbb{S}_{j}^{Inter} = \left\{(s_{1,j}, s_{2,j}, ..., s_{N,j}) : s_{i,j} \in \{0, 1\}, i = 1, 2, ..., N\right\}$. Again, the number of states for j^{th} location is 2^N which increases exponentially with N. Therefore, to reduce the complexity in verification, we here develop an analytical model of inter-network cooperation for $N = 2$.

Number of distinct states in this case is equal to four, which are denoted as, $A = (1, 1)$, $B = (0, 1)$, $C = (1, 0)$ and $D = (0, 0)$. The two digits in the states denote the operating modes of eNB from network 1 and 2 respectively. The state probabilities at j^{th} location are denoted by a vector $\mathbf{P_j^{S,Inter}} = [P_j^A,\ P_j^B,\ P_j^C,\ P_j^D]$, where P_j^A is the probability that the system is in state A. For convenience, we, once again, have omitted the time index here. Transition diagram for the system is shown in Fig. 3 and the corresponding transition matrix is given by, $\prod_j = \left[\mathbf{T_j^A},\ \mathbf{T_j^B},\ \mathbf{T_j^C},\ \mathbf{T_j^D}\right],\ \forall j, \forall t$. Here, $\mathbf{T_j^A} = [P_{AA},\ P_{BA},\ P_{CA}, P_{DA}]^T$, $\mathbf{T_j^B} = [P_{AB}, P_{BB},\ P_{CB},\ P_{DB}]^T$, $\mathbf{T_j^C} = [P_{AC},\ P_{BC},\ P_{CC},\ P_{DC}]^T$, $\mathbf{T_j^D} = [P_{AD},\ P_{BD},\ P_{CD},\ P_{DD}]^T$. We can then derive as below,

$$\left.\begin{aligned}
&P_{AB} = \left[Pr\left\{\mathcal{L}_{1,j} < \vartheta_{1,j}\right\} + Pr\left\{\mathcal{L}_{1,j} \geq \omega_{1,j}\right\}\right] \times Pr\left\{\mathcal{L}_{1,j} + \mathcal{L}_{2,j} < \varepsilon_{2,j}\right\} \\
&P_{AC} = Pr\left\{\vartheta_{1,j} \leq \mathcal{L}_{1,j} < \omega_{1,j}\right\} \times Pr\left\{\mathcal{L}_{1,j} + \mathcal{L}_{2,j} < \varepsilon_{1,j}\right\} \times Pr\left\{\mathcal{L}_{2,j} \geq \omega_{2,j}\right\} \\
&P_{BA} = Pr\left\{\mathcal{L}_{1,j} + \mathcal{L}_{2,j} \geq \varepsilon_{2,j}\right\}, \quad P_{BC} = Pr\left\{\mathcal{L}_{1,j} + \mathcal{L}_{2,j} < \varepsilon_{1,j}\right\} \times Pr\left\{\mathcal{L}_{2,j} \geq \omega_{2,j}\right\} \\
&P_{AA} = 1 - P_{AB} - P_{AC} - P_{AD}, P_{BB} = 1 - P_{BA} - P_{BC} - P_{BD}, P_{CC} = 1 - P_{CA} - P_{CB} - P_{CD} \\
&P_{CA} = P_{BA}, P_{CB} = P_{AB}, P_{AD} = P_{BD} = P_{CD} = P_{DA} = P_{DB} = P_{DC} = P_{DD} = 0
\end{aligned}\right\} \tag{16}$$

Then, the state probabilities for j^{th} location at time t is given by,

$$\mathbf{P_j^{S,Inter}} = \mathbf{P_j^{S,\Delta}} \prod\nolimits_j, \ \forall j, \forall t \tag{17}$$

where, $\mathbf{P_j^{S,\Delta}} = \left[P_j^{A,\Delta}, \ P_j^{B,\Delta}, \ P_j^{C,\Delta}, \ P_j^{D,\Delta}\right]$ is the state probability vector $\mathbf{P_j^{S,Inter}}$ at time $(t - \Delta)$. Initial state probability vector $\mathbf{P_j^{S,Inter}} = [1, 0, 0, 0], \ \forall t \leq 0, \forall j$. Then we can write,

$$Pr\left\{\mathcal{B}_{1,j} \text{ sleeps at time } t\right\} = P_{1,j}^{S,Inter} = \mathbf{P_j^{S,\Delta}} \cdot \left(\mathbf{T_j^B}\right)^T, \ \forall j, \forall t \tag{18}$$

$$\text{Similarly, } \ P_{2,j}^{S,Inter} = \mathbf{P_j^{S,\Delta}} \cdot \left(\mathbf{T_j^C}\right)^T, \ \forall j, \forall t \tag{19}$$

Conditional probabilities $P_{i,j}^{S,Inter}|_\alpha, i = 1, 2$ conditioned on α can then be simplified as below,

$$P_{1,j}^{S,Inter}|_\alpha = \left[P_j^{A,\Delta} + P_j^{C,\Delta}\right](1 - Q_1 + Q_2)(1 - Q_5) + P_j^{B,\Delta}\left[1 - Q_3(1 - Q_4) - Q_5\right] \tag{20}$$

$$P_{2,j}^{S,Inter}|_\alpha = \left[P_j^{A,\Delta}(Q_1 - Q_2) + P_j^{B,\Delta}\right] Q_3(1 - Q_4) + P_j^{C,\Delta}\left[1 - (1 - Q1 + Q_2)(1 - Q_5) - Q_4\right] \tag{21}$$

$$\left.\begin{aligned}
&\text{where, } \ Q_1 = Q\left(\frac{\frac{\vartheta_{1,j}}{\alpha f_{1,j}(t)} - \mu_{x_{1,j}}}{\sqrt{\sigma_{x_{1,j}}^2}}\right), \quad Q_2 = Q\left(\frac{\frac{\omega_{1,j}}{\alpha f_{1,j}(t)} - \mu_{x_{1,j}}}{\sqrt{\sigma_{x_{1,j}}^2}}\right), \quad Q_3 = Q\left(\frac{\frac{\omega_{2,j}}{\alpha f_{2,j}(t)} - \mu_{x_{2,j}}}{\sqrt{\sigma_{x_{2,j}}^2}}\right) \\
&Q_4 = Q\left(\frac{\varepsilon_{1,j} - \mu_{z_{N_i=2,j}}}{\sqrt{\sigma_{z_{N_i=2,j}}^2}}\right) \quad \text{and} \quad Q_5 = Q\left(\frac{\varepsilon_{2,j} - \mu_{z_{N_i,j}}}{\sqrt{\sigma_{z_{N_i,j}}^2}}\right)
\end{aligned}\right\} \tag{22}$$

Please refer to the Appendix for the derivation of the expressions in (22). $N_i = 2$ and $K_{i,j} = 1, \forall i$ are used for (22). Then, for location j at time t, we can write,

$$P_{i,j}^{S,Inter}(t) = \frac{1}{b - a} \int_a^b P_{i,j}^{S,Inter}|_\alpha \ d\alpha, \ \ i = 1, 2 \tag{23}$$

Thus, average sleeping probability of an eNB in the combined network can be given by,

$$P_{avg}^{S,Inter} = \left[\frac{1}{N_i N T} \sum_{i=1}^{N} \sum_{j=1}^{N_i} \int_0^T P_{i,j}^{S,Inter}(t) dt\right] \times 100\% \tag{24}$$

C. Joint Cooperation

Under the proposed joint cooperation scheme, switching of $\mathcal{B}_{i,j}$ from active to sleep mode and vice versa might result from either the intra-network cooperation or the internetwork cooperation.

Therefore, at time t, the probability of sleeping of $\mathcal{B}_{i,j}$ can be given by,

$$P_{i,j}^{S,Joint}(t) = \frac{1}{b-a}\int_a^b \left[P_{i,j}^{S,Intra}(t)|_\alpha + P_{i,j}^{S,Inter}(t)|_\alpha - P_{i,j}^{S,Intra}(t)|_\alpha \times P_{i,j}^{S,Inter}(t)|_\alpha\right] d\alpha,\ \ \forall i, \forall j, \forall t \tag{25}$$

Then averaging over time t, all eNBs and all E-UTRANs, overall probability that an eNB sleeps in the combined network can be given by,

$$P_{avg}^{S,Joint} = \left[\frac{1}{N_i NT}\sum_{i=1}^{N}\sum_{j=1}^{N_i}\int_0^T P_{i,j}^{S,Joint}(t)dt\right] \times 100\% \tag{26}$$

VI. Simulation, Results and Discussion

A. Simulation Setup

For evaluating the proposed energy saving cooperation techniques, a scenario of multiple co-located LTE E-UTRANs is used as the simulation platform. Each of the networks covers a geographical area using $N_i = 50$, hexagonal shaped macro cells of radius equal to 1 km. For the E-UTRANs, carrier frequency = 2.0 GHz and channel bandwidth (BW) = 20 MHz are assumed. This corresponds to 18 MHz transmission BW and 100 PRBs each of 180 kHz BW. 1/2-QPSK is assumed as the modulation scheme. WINNER+ non-line-of-sight (NLOS) urban macro-cell channel model has been considered [33]. Link budget parameters, eNB transmit power = 43 dBm, eNB antenna height = 25 m, MS antenna height = 1.5 m, eNB antenna gain = 18 dB, MS antenna gain = 0 dB, eNB cyclic combining gain = 3 dB, eNB feeder loss = 6 dB, eNB noise figure (NF) = 4 dB; MS NF = 6 dB, cell interference margin = 6 dB, multiple-input multiple-output (MIMO) gain = 3.5 dB, minimum downlink SINR = 4.3 dB, shadow fading margin = 8 dB and Gaussian noise power density = -174 dBm/Hz are used for simulations.

We assume that in the original network, eNB $\mathcal{B}_{i,j}, \forall i, \forall j$ provides $U_{i,j} = 2$ classes of connection-oriented constant bit rate services requiring $\eta_{i,j}^{(1)} = 1$ and $\eta_{i,j}^{(2)} = 2$ PRBs respectively. For the convenience, constant call duration $h_{i,j}^{(1)} = 3$ minutes and $h_{i,j}^{(2)} = 5$ minutes are assumed. Traffic generation rates are $\lambda_{i,j}^{(1)} = 13.9$ call/min and $\lambda_{i,j}^{(2)} = 4$ call/min respectively. When $\alpha = 1.0$, this settings results in 1% and 2% peak-time call blocking probabilities for class 1 and 2 respectively. It also corresponds to a peak-time load $\mathcal{L}_P \approx 82$ PRBs. Rate functions shown in Fig. 2 are used for generating time-inhomogeneous traffic. For time-inhomogeneous traffic, two traffic scenarios - S1 and S2, are simulated. S1 simulates the temporal variation only, whereas, S2 simulates both temporal and spatial variations of traffic generations. Users are uniformly distributed in the networks, while the total number of users may vary among eNBs and the networks (i.e., when $\alpha_{i,j} \neq 1$).

We have evaluated our system for both the CEC and NEP type eNBs using $g_{i,j} = 21.45$ and $h_{i,j} = 354.44, \forall i, \forall j$ [26]. Depending on the designs of eNB hardware, sleep mode power $P_{i,j}^{Sleep}$ of

$\mathcal{B}_{i,j}$ may vary. Therefore, to cover different types of eNBs, for each of the two models, two different settings are considered for $P_{i,j}^{Sleep}$. For CEC model, the two settings are 0 watt and h watt, which are designated as CEC1 and CEC2 respectively. While, for NEP model, the settings are 0 watt and δh watt, and named as NEP1 and NEP2 respectively. Moreover, unless otherwise specified, presented results correspond to a network comprises of two E-UTRANs (i.e.,$N = 2$) with traffic scenario S1, rate function $f_2(t)$, $\delta_{i,j} = 0.7, \alpha_{i,j} = 1.0, \vartheta_{i,j} = \vartheta, \omega_{i,j} = \omega, \varepsilon_{i,j} = \varepsilon, \forall i, \forall j$ and $t_{Sw}^{AS} = t_{Sw}^{SA} = t_B^{AS} = 30$ sec [27].

B. Sleeping Probability, Transmit Power, Switching in eNBs and Network Capacity Utilization

Analytical and simulation results of average sleeping probabilities of eNBs per day P_S is presented in Fig. 4 and Fig. 5. For Fig. 4, $\omega = 0.7\mathcal{L}_P$ and $\varepsilon = 0.9\mathcal{L}_P$, while for Fig. 5, $\vartheta = 0.4\mathcal{L}_P$ and $\omega = 0.6\mathcal{L}_P$ are used. Both the figures show increasing trends in P_S for all the three cooperation techniques. Higher value of ϑ implies a higher number of eNBs have the probability of having traffic load less than ϑ and thus, higher number of eNBs may distribute their traffic and switch from active to sleep mode. This results in higher P_S as evident from Fig. 4. Similarly, a higher value of ε implies that an eNB can accept higher amount of traffic from other eNBs, which allows higher number of eNBs to sleep resulting in higher P_S as seen in Fig. 5. Also, out of the three cooperation techniques, eNBs under joint cooperation has the highest probability to switch to sleep mode. In addition, P_S corresponding to $\alpha \sim U[0.5, 1.0]$ is also shown in Fig. 5. Because of the lower traffic in eNBs, this setting results in much higher P_S than that of with $\alpha = 1.0$. Finally, from both the figures, it is evident that the analytical results closely follow the simulation results which validates our simulation models.

Average additional transmit power, $\mathcal{P}_{Tx}^{avg}$ and switching statistics per eNB, $\mathcal{N}_{Sw}$ are demonstrated in Fig. 6(a) and (b) respectively. Here, $\omega = 0.7\mathcal{L}_P$ and $\varepsilon = 0.9\mathcal{L}_P$ are used. From Fig. 6(a), it is seen that a network with traffic shaping rate function $f_2(t)$ requires higher $\mathcal{P}_{Tx}^{avg}$ than that of a network having rate function $f_1(t)$. A network having $f_2(t)$ corresponds to higher traffic generation. In such a network, active eNBs share higher amount of traffic generated in the sleeping eNBs, which results in higher $\mathcal{P}_{Tx}^{avg}$. In addition, for both the rate functions, $\mathcal{P}_{Tx}^{avg}$ is significantly higher in S2 ($> 23\%$) than in S1 ($< 5\%$). On the other hand, from Fig. 6(b), it is evident that networks under intra-network cooperation has the lowest number of switching, while highest number of switching is observed in joint cooperation. Similar to the additional transmit power, here again, number of switching is substantially higher in S2 than in S1. For instance, under joint cooperation, it is 20~25% in S2, while 4~7% for S1.

Fig. 7 illustrates NCUI evaluated under both S1 and S2. Switching thresholds are same as those used for Fig. 4. Increasing trend similar to P_S (in Fig. 4) is also manifested in NCUI. Higher value of P_S implies that the same amount of traffic is being served by fewer number of active eNBs, resulting in higher efficiency in network capacity utilization. Thus, our cooperative schemes can significantly improve the network CUE. It is also observed that the network under S2 can have significantly higher NCUI than that in S1. In S2, due to both temporal and spatial variation of traffic generation, peak traffic times vary among eNBs. Consequently, at any time of a day, total traffic of the network remains lower than its total capacity. Therefore, over the day, there are always some sleeping eNBs resulting in higher P_S and higher NCUI as well.

C. Net Energy Savings

1) Time-Inhomogeneous Traffic Scenario: Average net energy savings per day under joint cooperation has been presented in Fig. 8 and Fig. 9. For comparison purpose, P_S is also included in the figures. Impact of switching threshold, number of E-UTRANs, rate functions, power consumption profiles of eNBs and traffic distributions are demonstrated in detail in the two figures. For both the figures, $\omega = 0.7\mathcal{L}_P$ and $\varepsilon = 0.9\mathcal{L}_P$ are used in the simulations.

In S1, as shown in Fig. 8, net energy savings has an increasing trend with ϑ. Comparing Fig. 8(a) and Fig. 9(b), we can note that in S1, savings is slightly less than P_S; while the difference is much bigger in S2. This is due to the much higher additional transmit power and switching of eNBs in S2, than those of S1 as explained in Section VI-B. Furthermore, it is seen that with the increase of the number of cooperating networks from 2 to 4, extent of savings also increases. In addition, a network with $f_1(t)$ saves higher than a network with $f_2(t)$ due to the lower traffic load in the former one as demonstrated in Fig. 2.

On the other hand, substantial dependence of net energy savings on the power models of eNBs is clearly evident from the two figures. For example, CEC1 and NEP1 models are saving much higher than CEC2 and NEP2 respectively. This is because, eNBs of CEC1 and NEP1 models do not consume any energy in sleep mode, while the other two do. On the other hand, since eNBs of NEP models, to some extent, are technologically optimized for saving energy, in general, NEP models save lower than or equal to that of CEC models.

Fig. 10 demonstrates the impact of eNB model parameter δ on net energy savings. $\vartheta = 0.5\mathcal{L}_P$, $\omega = 0.7\mathcal{L}_P, \varepsilon = 0.9\mathcal{L}_P$ and $N = 4$ are used for simulations. Corresponding P_S is also shown. As seen, although many eNBs sleep at $\delta = 0$, there is no energy savings from any of the cooperation techniques. Because, $\delta = 0$ is an ideal case, which implies that eNBs are of FEP model and hence, energy consumption changes linearly with the traffic load. Thus, switching off eNBs does not result

in any additional energy savings. With the increase of δ, eNBs become more non-energy proportional type and therefore, proposed cooperation techniques save higher and higher. Also, with the increase of δ, the gap between the savings from NEP1 and NEP2 models widens.

2) Time-Homogeneous Traffic Scenario: Net energy savings along with P_S under time- homogeneous traffic generation is also evaluated and presented for CEC1 model in Fig. 11. The network is simulated using, $\vartheta = 0.5\mathcal{L}_P$, $\omega = 0.5\mathcal{L}_P$ and $\varepsilon = 1.0\mathcal{L}_P$. As seen, with the increase of traffic load in eNBs, P_S and correspondingly energy savings is dropping. The drop in P_S as well as in savings is gradual in the lower range of network load (upto 40%) and thereafter drops sharply. In low traffic situation, very little additional transmit power is required and the number of switching is very few. Therefore, the savings is very close to P_S in all the three cooperation techniques. However, as the traffic increases, both the additional power requirement and the number of switching increase significantly, which substantially reduces the savings. Energy savings can even become negative at higher loads (viz., at 60% load).

D. Optimization of Savings

Using exhaustive search technique, we have evaluated the optimal energy savings and corresponding parameters. $\left(P_i^B\right)_{Th}$ equal to the original network and $\mathcal{N}_{Sw}^{Th} = 5\%$ are used for the optimizations. Optimal savings with the number of cooperating networks N for CEC1 model under time-inhomogeneous traffic scenario has been demonstrated in Fig. 12. Savings corresponding to $N = 1$ represents the savings from intra-network cooperation. As observed, energy savings from P1 and P2 optimization approaches is increasing with N. In contrast, for $N = 6$ and beyond, the trend is quite different for P3 optimization, where no savings is possible. As, average number of switching also increases with the increase of N and becomes greater than 5% for $N = 6$, no savings is achieved from P3. It can also be noted that upto $N = 4$, P1 optimization gives the highest savings, which has no restriction on the number of switching. On the other hand, P2 generates the lowest savings as it minimizes the number of switching as well. Whereas, savings from P3 varies between the savings from P1 and P2.

Cumulative distribution function (CDF) of sleeping time per day of eNBs under joint cooperation is demonstrated in Fig. 13. Switching thresholds ϑ, ω and ε used for the simulations are determined from P1 optimization of CEC1 model. As expected, eNBs under the higher number of cooperating networks sleep for longer time. For example, for $\alpha = 1.0$, sleep times varies in the range of [0.9, 15.6] hours, [4.25, 16.7] hours and [6.3, 17.4] hours for $N = 2, 4$ and 6 respectively. Also, the intersection of the CDFs with the abscissa indicates that under joint cooperation, all eNBs in the cooperating networks can stay in sleep mode for a certain duration over a day and save energy. With

lower traffic in the network, eNBs can sleep longer times as evident from the CDFs corresponding to $\alpha \sim U[0.3, 0.8]$.

E. Comparison with Related Works

Due to the absence of any unique performance metric for evaluating energy saving techniques and varieties in the considered network topologies, it is difficult to compare one research with another. In addition, research level in the arena of energy saving cellular networks is still in the early stage and hence, most of the published papers lack in concrete system modeling. Nevertheless, here we have compared our proposed techniques with four other recently published results in [11], [12], [20] and [21], which is presented as a bar chart in Fig. 14. Oh *et al.* [11] and Zhisheng *et al.* [12] estimated savings from switching off BTSs in a single network. In contrast, Ismail *et al.* [20] and Marsan *et al.* [21] presented the results corresponding to the cooperation among multiple networks.

From the bar chart, it is clear that our proposed scheme can save higher from the respective schemes. In addition, all of these works clearly lack in capturing the impact of switching transient and the realistic power consumption models of eNBs. Furthermore, except [12], the other three schemes are of centralized type and have not presented any algorithm. In contrast, our proposed techniques and algorithms are of distributed and self-organizing type. While, due to the self-organizing interaction among eNBs, our techniques can increase the computational load of eNBs by little amount. However, due to the already started paradigm shift from manually managed network types to SONs, our proposed techniques are compatible for the future networks.

VII. Conclusion

In this paper, three different energy saving eNB-centric cooperation mechanisms for self-organizing LTE networks have been thoroughly investigated. Under the proposed techniques, traffic-aware mutual cooperation among eNBs is employed for dynamically reconfiguring E-UTRAN(s) with the reduced number of active eNBs for saving energy. Comprehensive simulations under wide range of network scenarios, traffic distributions and eNB power profiles are carried out. Simulation results have shown that a significant amount of energy savings is possible, while maintaining QoS. A network taking part in joint cooperation can gain much higher savings than that of intra-network and inter-network cooperation only. It is found that although a higher number of eNBs can sleep in a network having both temporal and spatial variation in traffic, net savings is much less due to additional transmit power and higher number of switching. On the other hand, power consumption profiles of eNBs are found to have tremendous impact on the achievable savings. An eNB with CEC model can save more compared to that of NEP model. In addition, network capacity utilization,

number of switching, additional transmit power and sleep time of eNBs under the proposed system are also investigated. Furthermore, results from the analytical models have shown close proximity with the simulation results, which has validated the simulation models. A comparison of our system performance with the other published results is also provided, which has established the supremacy of our system.

Appendix

Without losing the generality, we can use $f_{i,j}^{(u)}(t) = f_{i,j}(t), \forall u$. We also assume that $\alpha_{i,j} \geq 0, \forall i, \forall j$ are i.i.d. uniform RVs over a range $[a,\ b]$ and thus, we can write, $\alpha_{i,j} = \alpha,\ \forall i, \forall j$. Hence,

$$Pr\left\{\sum_{i=1}^{N_i} K_{i,j}\mathcal{L}_{i,j}(t) < \Theta|_\alpha\right\} = Pr\left\{\sum_{i=1}^{N_i}\sum_{u=1}^{U_{i,j}} K_{i,j}f_{i,j}(t)\rho_{i,j}^{(u)}h_{i,j}^{(u)}\eta_{i,j}^{(u)} < \frac{\Theta}{\alpha}|_\alpha\right\}$$

$$= Pr\left\{Z_{N_i,j} < \frac{\frac{\Theta}{\alpha} - \mu_{z_{N_i,j}}}{\sqrt{\sigma^2_{z_{N_i,j}}}}|_\alpha\right\} = 1 - Pr\left\{Z_{N_i,j} \geq \frac{\frac{\Theta}{\alpha} - \mu_{z_{N_i,j}}}{\sqrt{\sigma^2_{z_{N_i,j}}}}|_\alpha\right\} = 1 - Q\left(\frac{\frac{\Theta}{\alpha} - \mu_{z_{N_i,j}}}{\sqrt{\sigma^2_{z_{N_i,j}}}}\right),\ \forall j \tag{27}$$

where, $Z_{N_i,j}$ is approximated by a Normal RV with zero mean and unit variance; Θ and $K_{i,j}, \forall i, \forall j$ are constants. Here, $\mu_{z_{N_i,j}}$ and $\sigma^2_{z_{N_i,j}}$ are given by,

$$\mu_{z_{N_i,j}} = \sum_{i=1}^{N_i}\sum_{u=1}^{U_{i,j}} K_{i,j}f_{i,j}(t)\lambda_{i,j}^{(u)}h_{i,j}^{(u)}\eta_{i,j}^{(u)} \text{ and } \sigma^2_{z_{N_i,j}} = \sum_{i=1}^{N_i}\sum_{u=1}^{U_{i,j}}\left(K_{i,j}\right)^2 f_{i,j}^2(t)\lambda_{i,j}^{(u)}\left(h_{i,j}^{(u)}\right)^2\left(\eta_{i,j}^{(u)}\right)^2,\ \forall j \tag{28}$$

As a special case, for a particular eNB $\mathcal{B}_{i,j}$, by setting $K_{i,j} = 1$ and $\Theta = \vartheta_{i,j}$, we can write,

$$Pr\left\{\mathcal{L}_{i,j}(t) < \vartheta_{i,j}|_\alpha\right\} = Pr\left\{\sum_{u=1}^{U_{i,j}}\rho_{i,j}^{(u)}h_{i,j}^{(u)}\eta_{i,j}^{(u)} < \frac{\vartheta_{i,j}}{\alpha f_{i,j}(t)}\right\} = 1 - Q\left(\frac{\frac{\vartheta_{i,j}}{\alpha f_{i,j}(t)} - \mu_{x_{i,j}}}{\sqrt{\sigma^2_{x_{i,j}}}}\right) \tag{29}$$

where, $\mu_{x_{i,j}} = \sum_{u=1}^{U_{i,j}}\lambda_{i,j}^{(u)}h_{i,j}^{(u)}\eta_{i,j}^{(u)}$ and $\sigma^2_{x_{i,j}} = \sum_{u=1}^{U_{i,j}}\lambda_{i,j}^{(u)}\left(h_{i,j}^{(u)}\right)^2\left(\eta_{i,j}^{(u)}\right)^2$.

$$\text{Similarly, } Pr\left\{\mathcal{L}_{i,j}(t) \geq \omega_{i,j}|_\alpha\right\} = 1 - Pr\left\{\mathcal{L}_{i,j}(t) < \omega_{i,j}|_\alpha\right\} = Q\left(\frac{\frac{\omega_{i,j}}{\alpha f_{i,j}(t)} - \mu_{x_{i,j}}}{\sqrt{\sigma^2_{x_{i,j}}}}\right) \tag{30}$$

$$Pr\left\{\vartheta_{i,j} \leq \mathcal{L}_{i,j}(t) < \omega_{i,j}|_\alpha\right\} = Q\left(\frac{\frac{\vartheta_{i,j}}{\alpha f_{i,j}(t)} - \mu_{x_{i,j}}}{\sqrt{\sigma^2_{x_{i,j}}}}\right) - Q\left(\frac{\frac{\omega_{i,j}}{\alpha f_{i,j}(t)} - \mu_{x_{i,j}}}{\sqrt{\sigma^2_{x_{i,j}}}}\right) \tag{31}$$

$$\text{Again, } Pr\left\{(\varepsilon_{i,j}^{n,k} - \mathcal{L}_{i,j}^{n,k}(t) > \beta_{i,j}^{n,k}\mathcal{L}_{i,j}(t)|_\alpha\right\} = Pr\left\{\beta_{i,j}^{n,k}\mathcal{L}_{i,j}(t) + \mathcal{L}_{i,j}^{(n,k)}(t) < \varepsilon_{i,j}^{n,k}|_\alpha\right\}$$

$$= Pr\left\{\alpha\beta_{i,j}^{n,k}f_{i,j}(t)\sum_{u=1}^{U_{i,j}}\rho_{i,j}^{(u)}h_{i,j}^{(u)}\eta_{i,j}^{(u)} + \alpha f_{i,j}^{n,k}(t)\sum_{u=1}^{U_{i,j}^{n,k}}\rho_{i,j}^{n,k(u)}h_{i,j}^{n,k(u)}\eta_{i,j}^{n,k(u)} < \varepsilon_{i,j}^{n,k}|_\alpha\right\}$$

$$= Pr\left\{ Y_{i,j} < \frac{\varepsilon_{i,j}^{n,k} - \mu_{y_{i,j}}}{\sqrt{\sigma_{y_{i,j}}^2}} \right\} = 1 - Q\left(\frac{\varepsilon_{i,j}^{n,k} - \mu_{y_{i,j}}}{\sqrt{\sigma_{y_{i,j}}^2}} \right) \tag{32}$$

where, $Y_{i,j}$ is a Normal RV with zero mean and unit variance. $\mu_{y_{i,j}}$ and $\sigma_{y_{i,j}}^2$ are given by,

$$\mu_{y_{i,j}} = \alpha \beta_{i,j}^{n,k} f_{i,j}(t) \sum_{u=1}^{U_{i,j}} \lambda_{i,j}^{(u)} h_{i,j}^{(u)} \eta_{i,j}^{(u)} + \alpha f_{i,j}^{n,k}(t) \sum_{u=1}^{U_{i,j}^{n,k}} \lambda_{i,j}^{n,k(u)} h_{i,j}^{n,k(u)} \eta_{i,j}^{n,k(u)} \tag{33}$$

$$\sigma_{y_{i,j}}^2 = \alpha^2 (\beta_{i,j}^{n,k})^2 f_{i,j}^2(t) \sum_{u=1}^{U_{i,j}} \lambda_{i,j}^{(u)} \left(h_{i,j}^{(u)} \right)^2 \left(\eta_{i,j}^{(u)} \right)^2 + \alpha^2 \left(f_{i,j}^{n,k}(t) \right)^2 \sum_{u=1}^{U_{i,j}^{n,k}} \lambda_{i,j}^{n,k(u)} \left(h_{i,j}^{n,k(u)} \right)^2 \left(\eta_{i,j}^{n,k(u)} \right)^2 \tag{34}$$

Acknowledgment

This work is supported by the Australian Research Council under the Discovery Project (DP 1096276).

References

[1] R. Bolla *et al.*, "Energy Efficiency in the Future Internet: a Survey of Existing Approaches and Trends in Energy-Aware Fixed Network Infrastructure," *IEEE Comm. Surveys and Tutorials*, vol. 13, no. 2, pp. 223-244, 2011.

[2] A. Fehske *et al.*, "The global footprint of mobile communications: The ecological and economic perspective," *IEEE Communications Magazine*, vol. 49, no. 8, pp. 55-62, Aug 2011.

[3] Kyuho *et al.*, "Base Station Operation and User Association Mechanisms for Energy-Delay Tradeoffs in Green Cellular Networks," *IEEE Journal on Selected Areas in Communications*, vol. 29, no. 8, pp. 1525-1536, Sep 2011.

[4] Sallent *et al.*, "A Roadmap from UMTS Optimization to LTE Self-optimization," *IEEE Communications Magazine*, vol. 49, no. 6, pp. 172-182, Jun 2011.

[5] 3GPP TR 36.902 ver. 9.3.1 Rel. 9, "Evolved Universal Terrestrial Radio Access Network (E-UTRAN); Self-Configuring and Self-Optimizing Network (SON): Use Cases and Solutions," Technical Report, 2011.

[6] WMF-T33-120-R016v01, "Architecture, Detailed Protocols and Procedures: Self-Organizing Networks," WiMAX Forum Network Architecture, Jun 2010.

[7] Z. Hasan *et al.*, "Green Cellular Networks: A Survey, Some Research Issues and Challenges," *IEEE Communications Surveys and Tutorials*, vol. 13, no. 4, pp. 524-540, Fourth Quarter 2011.

[8] M. A. Marsan *et al.*, "Optimal Energy Savings in Cellular Access Networks," *Proc. Workshop on Green Comm. in conjunction with IEEE ICC*, Dresden, Germany, pp. 1-5, Jun 2009.

[9] F. Han *et al.*, "Energy-Efficient Cellular Network Operation via Base Station Cooperation," *Proc. of Int. Conf. on Comm.(ICC)*, pp. 5885-5889, Ottawa, Canada, Jun 2012.

[10] S. Zhou *et al.*, "Green Mobile Access Network with Dynamic Base Station Energy Saving," *Proc. ACM Int. Conf. on Mobile Computing and Networking*, Beijing, China, pp. 1-3, Sep 2009.

[11] E. Oh *et al.*, "Energy Savings through Dynamic Base Station Switching in Cellular Wireless Access Networks," *Proc. IEEE Global Telecomm. Conf. (GLOBECOM)*, pp. 1-5, Dec. 2010.

[12] Z. Niu *et al.*, "Cell Zooming for Cost-Efficient Green Cellular Networks," *IEEE Comm. Magazine*, vol. 48, no. 11, pp. 74-79, Nov 2010.

[13] D. Tipper *et al.*, "Dimming Cellular Networks, *in Proc. of IEEE Global Telecomm. Conf. (GLOBECOM)*, Miami, USA, pp. 1-6, Dec 2010.

[14] K. Son *et al.*, "Energy-Aware Hierarchical Cell Configuration: From Deployment to Operation," *Proc. IEEE INFOCOM Workshop on Computer Communications*, pp. 289-294, Apr 2011.

[15] H. Leem *et al.*, "The Effects of Cell Size on Energy Saving, System Capacity, and Per-Energy Capacity," *Proc. IEEE Wireless Comm. and Net. Conf. (WCNC)*, Sydney, Australia, pp. 1-6, Apr 2010.

[16] I. Humar *et al.*, "Rethinking Energy Efficiency Models of Cellular Networks with Embodied Energy," IEEE Network Magazine, vol.25, no.2, pp.40-49, Mar-Apr 2011.

[17] Z. Niu *et al.*, "Energy-Aware Network Planning for Wireless Cellular System with Inter-Cell Cooperation," *IEEE Transactions on Wireless Communications*, vol. 11, no. 4, pp. 1412-1423, Apr 2012.

[18] M. F. Hossain *et al.*, "Two Level Cooperation for Energy Efficiency in Multi-RAN Cellular Network Environment," *Proc. IEEE Wireless Comm. and Net. Conf. (WCNC)*, pp. 2493-2497, Paris, France, Apr 2012.

[19] E. Oh *et al.*, "Toward Dynamic Energy-Efficient Operation of Cellular Network Infrastructure," *IEEE Comm. Magazine*, vol. 49, no. 6, pp. 56-61, Jun 2011.

[20] M. Ismail *et al.*, "Network Cooperation for Energy Saving in Green Radio Communications," *IEEE Wireless Communications*, vol. 18, no. 5, pp. 76-81, Oct 2011.

[21] M. A. Marsan *et al.*, "Energy Efficient Wireless Internet Access with Cooperative Cellular Networks," *Elsevier Journal of Comp. Comm.*, vol. 55, no. 2, pp. 386-398, Feb 2011.

[22] U. Paul *et al.*, "Understanding Traffic Dynamics in Cellular Data Networks," *Proc. IEEE INFOCOM*, pp. 882-890, Apr 2011.

[23] M. Z. Shafiq *et al.*, "Characterizing and Modeling Internet Traffic Dynamics of Cellular Devices," *Proc. ACM SIGMETRICS*, pp. 305-316, Jun 2011.

[24] L. M. Correria *et al.*, "Challenges and Enabling Technologies for Energy Aware Mobile Radio Networks," *IEEE Comm. Magazine*, vol. 48, no. 11, pp. 66-72, Nov 2010.

[25] O. Arnold *et al.*, "Power Consumption Modeling of Different Base Station Types in Heterogeneous Cellular Networks," *Proc. of Future Network and Mobile Summit*, Florence, Italy, Jun 2010.

[26] Richter *et al.*, "Energy Efficiency Aspects of Base Station Deployment Strategies for Cellular Networks," *Proc. IEEE Vehicular Technology Conference (VTC)*, pp. 1-5, USA, Sep 2009.

[27] A. Conte *et al.*, "Cell Wilting and Blossoming for Energy Efficiency," *IEEE Wireless Comm.*, vol. 18, no. 5, pp. 50-57, Oct 2011.

[28] M. Deruyck *et al.*, "Modelling and Optimization of Power Consumption in Wireless Access Networks," *Elsevier Journal of Comp. Comm.*, vol. 34, no. 17, pp. 2036-2046, 2011.

[29] A. L. Stolyar *et al.*, "Self-Organizing Dynamic Fractional Frequency Reuse for Best-Effort Traffic through Distributed Inter-Cell Coordination," *Proc. IEEE INFOCOM*, pp. 1287-1295, Apr 2009.

[30] M. Xuehong *et al.*, "Adaptive Soft Frequency Reuse for Inter-Cell Interference Coordination in SC-FDMA Based 3GPP LTE Uplinks," *Proc. IEEE Global Telecomm. Conf. (GLOBECOM)*, pp. 1-6, Nov -Dec 2008.

[31] S. Elayoubi *et al.*, "Performance Evaluation of Frequency Planning Schemes in OFDMA-Based Networks," *IEEE Transactions on Wireless Communications*, vol. 7, no. 5, pp. 1623-1633, May 2008.

[32] R. Bosisio *et al.*, "Interference Coordination Vs. Interference Randomization in Multicell 3GPP LTE System," *Proc. IEEE Wireless Comm. and Net. Conf. (WCNC)*, pp. 824-829, Mar-Apr 2008.

[33] Wireless World Initiative New Radio WINNER+, "D5.3: WINNER+ Final Channel Models," Jun 2010.

TABLE I: Summary of the notations used in the algorithm section

N	Number of cooperating networks	$u_{i,j}^{(k)}$	k^{th} acceptor of $\mathcal{B}_{i,j}$
$\mathcal{B}_{i,j}$	j^{th} eNB of i^{th} network	$v_{i,j}^{(k)}$	k^{th} shared eNB by $\mathcal{B}_{i,j}$
N_i	Number of eNBs in i^{th} network	$\mathcal{B}_{i,j}^{(k)}$	k^{th} candidate eNB of $\mathcal{B}_{i,j}$
$N_{\mathcal{B}_{i,j}}$	Number of neighbors of $\mathcal{B}_{i,j}$	$\mathcal{L}_{i,j}^{(k)}$	Traffic load of $\mathcal{B}_{i,j}^{(k)}$
$\mathcal{L}_{i,j}$	Traffic load of $\mathcal{B}_{i,j}$	$s_{i,j}^{(k)}$	Operating mode of $\mathcal{B}_{i,j}^{(k)}$
$s_{i,j}$	operating mode of $\mathcal{B}_{i,j}$	$p_{i,j}^{(k)}$	Transmit power of $\mathcal{B}_{i,j}^{(k)}$
$p_{i,j}$	Transmit power of $\mathcal{B}_{i,j}$	$\mathbf{C}_{i,j}^{(k)}$, $\mathbb{D}_{i,j}$	Candidate set of $\mathcal{B}_{i,j}$
$\vartheta_{i,j}$	Low load threshold of $\mathcal{B}_{i,j}$	$C_{i,j}^{m,k}$	k^{th} eNB in $\mathbf{C}_{i,j}^{(m)}$
$\omega_{i,j}$	High load threshold of $\mathcal{B}_{i,j}$	$(\ .\ )_{i,j}^{*}$	Best set for $\mathcal{B}_{i,j}$
$\varepsilon_{i,j}$	Acceptance threshold of $\mathcal{B}_{i,j}$	$tf(\mathbf{B})$	Traffic matrix of eNB matrix $\mathbf{B}$
$\vartheta_{i,j}^{(k)}$, $\omega_{i,j}^{(k)}$, $\varepsilon_{i,j}^{(k)}$	Switching thresholds of $\mathcal{B}_{i,j}^{(k)}$	$\lvert\mathbf{A}\rvert$	Cardinality of vector $\mathbf{A}$

TABLE II: *(Intra-network Cooperation) Traffic Distribution of* $\mathcal{B}_{i,j}$ *if* $\mathcal{L}_{i,j} < \vartheta_{i,j}, \forall i, \forall j$

1:	Initialize $s_{i,j},\ p_{i,j},\ \mathcal{I}_{i,j}, \mathcal{A}_{i,j}, \mathcal{S}_{i,j}, \Psi_{i,j}, \mathbf{U}_{i,j}, \mathbf{V}_{i,j}, \mathbb{C}_{i,j}$
2:	**If** $s_{i,j} = 1,\ \mathcal{L}_{i,j} < \vartheta_{i,j},\ Z_{i,j} = 0$ and $\mathbb{C}_{i,j}^{a} \neq \emptyset$
3:	Find $\mathbf{F}_{i,j}^{*} \subseteq \mathbb{C}_{i,j}^{a}$
4:	**Elseif** $s_{i,j} = 1,\ \mathcal{L}_{i,j} < \vartheta_{i,j},\ Z_{i,j} \neq 0$ and $\mathbb{C}_{i,j}^{a} \neq \emptyset$
5:	Find $\mathbf{F}_{i,j}^{*} \subseteq \mathbb{C}_{i,j}^{a}$ such that $v_{i,j}^{(k)} \in \mathbf{F}_{i,j}^{*}, \forall k = 1, 2, ..., Z_{i,j}$
6:	**End If**
7:	**If** $\mathbf{F}_{i,j}^{*} \neq \emptyset$
8:	Set $s_{i,j}, p_{i,j}, \mathcal{L}_{i,j} = 0; \mathbf{U}_{i,j} = \mathbf{U}_{i,j} \cup \mathbf{F}_{i,j}^{*}; \mathbf{V}_{i,j} = \emptyset$
9:	Update $s_{l,m}, p_{l,m}, \mathcal{L}_{l,m}, \mathbf{U}_{l,m},\ \mathbf{V}_{l,m} \forall \mathcal{B}_{l,m} \in \mathbf{F}_{i,j}^{*}$
10:	**End If**

TABLE III: *(Intra-network Cooperation) Traffic Distribution of* $\mathcal{B}_{i,j}$ *if* $\mathcal{L}_{i,j} \geq \omega_{i,j}, \forall i, \forall j$

1:	Initialize $s_{i,j},\ p_{i,j},\ \mathcal{I}_{i,j}, \mathcal{A}_{i,j}, \mathcal{S}_{i,j}, \Psi_{i,j}, \mathbf{U}_{i,j}, \mathbf{V}_{i,j}, \mathbb{C}_{i,j}$
2:	**If** $s_{i,j} = 1,\ \mathcal{L}_{i,j} \geq \omega_{i,j},\ Z_{i,j} = 0$ and $\mathbb{C}_{i,j}^{a} \neq \emptyset$
3:	Find $\mathbf{F}_{i,j}^{*} \subseteq \mathbb{C}_{i,j}^{a}$
4:	**Elseif** $s_{i,j} = 1,\ \mathcal{L}_{i,j} \geq \omega_{i,j},\ Z_{i,j} \neq 0$ and $\mathbb{C}_{i,j}^{a} \neq \emptyset$
5:	Find $\mathbf{F}_{i,j}^{*} \subseteq \mathbb{C}_{i,j}^{a}$ such that $v_{i,j}^{(k)} \in \mathbf{F}_{i,j}^{*}, \forall k = 1, 2, ..., Z_{i,j}$

6:	**End If**
7:	**If** $\mathbf{F}^*_{i,j} \neq \emptyset$
8:	Set $s_{i,j}, p_{i,j}, \mathcal{L}_{i,j} = 0; \mathbf{U}_{i,j} = \mathbf{U}_{i,j} \cup \mathbf{F}^*_{i,j}; \mathbf{V}_{i,j} = \emptyset$
9:	Update $s_{l,m}, p_{l,m}, \mathcal{L}_{l,m}, \mathbf{U}_{l,m}, \mathbf{V}_{l,m}, \forall \mathcal{B}_{l,m} \in \mathbf{F}^*_{i,j}$
10:	Stop the algorithm
11:	**Else** Find $\mathbf{F}^*_{i,j} \subseteq \mathbb{C}^a_{i,j}$ for distributing $(\mathcal{L}_{i,j} - \omega_{i,j})$
12:	**If** $\mathbf{F}^*_{i,j} \neq \emptyset$
13:	Set $\mathcal{L}_{i,j} = \omega_{i,j}, \mathbf{U}_{i,j} = \mathbf{U}_{i,j} \cup \mathbf{F}^*_{i,j}$ and update $p_{i,j}$
14:	Update $\mathcal{L}_{l,m}, s_{l,m}, p_{l,m}, \mathbf{U}_{l,m}, \mathbf{V}_{l,m}, \forall \mathcal{B}_{l,m} \in \mathbf{F}^*_{i,j}$
15:	Stop the algorithm
16:	**End If**
17:	**End If**
18:	**If** $s_{i,j} = 1$, $\mathcal{L}_{i,j} \geq \omega_{i,j}$, $Z_{i,j} = 0$ and $\mathbb{C}^s_{i,j} \neq \emptyset$
19:	Find $\mathbf{H}^*_{i,j} \subseteq \mathbb{C}^s_{i,j}$
20:	**Elseif** $s_{i,j} = 1$, $\mathcal{L}_{i,j} \geq \omega_{i,j}$, $Z_{i,j} \neq 0$ and $\mathbb{C}^s_{i,j} \neq \emptyset$
21:	Find $\mathbf{H}^*_{i,j} \subseteq \mathbb{C}^s_{i,j}$ such that $v^{(k)}_{i,j} \in \mathbf{H}^*_{i,j}, \forall k = 1, 2, ..., Z_{i,j}$
22:	**End If**
23:	**If** $\mathbf{H}^*_{i,j} \neq \emptyset$
24:	Set $s_{i,j}, p_{i,j}, \mathcal{L}_{i,j} = 0; \mathbf{U}_{i,j} = \mathbf{U}_{i,j} \cup \mathbf{H}^*_{i,j}; \mathbf{V}_{i,j} = \emptyset$
25:	Update $s_{l,m}, p_{l,m}, \mathcal{L}_{l,m}, \mathbf{U}_{l,m}, \mathbf{V}_{l,m}, \forall \mathcal{B}_{l,m} \in \mathbf{H}^*_{i,j}$
26:	**Else** Find $\mathbf{H}^*_{i,j} \subseteq \mathbb{C}^s_{i,j}$ for distributing $(\mathcal{L}_{i,j} - \omega_{i,j})$
27:	**If** $\mathbf{H}^*_{i,j} \neq \emptyset$
28:	Set $\mathcal{L}_{i,j} = \omega_{i,j}, \mathbf{U}_{i,j} = \mathbf{U}_{i,j} \cup \mathbf{H}^*_{i,j}$ and update $p_{i,j}$
29:	Update $s_{l,m}, p_{l,m}, \mathcal{L}_{l,m}, \mathbf{U}_{l,m}, \mathbf{V}_{l,m}, \forall \mathcal{B}_{l,m} \in \mathbf{F}^*_{i,j}$
30:	**End If**
31:	**End If**

TABLE IV: *(Intra-network Cooperation) Selection Procedure of* $\mathbf{F}^*_{i,j}$ *for* $\mathcal{B}_{i,j}, \forall i, \forall j$

1:	Initialize $s_{i,j}, p_{i,j}, \mathcal{I}_{i,j}, \mathcal{A}_{i,j}, \mathcal{S}_{i,j}, \Psi_{i,j}, \mathbf{U}_{i,j}, \mathbf{V}_{i,j}, \mathbb{C}_{i,j}, \mathbb{C}^a_{i,j}, \mathbf{F}^*_{i,j}$
2:	Find $\mathbb{L} = tf(\mathbb{C}^a_{i,j})$ allocating $\mathcal{L}_{i,j}$ in each $\mathbf{F}^{(s)}_{i,j} \in \mathbb{C}^a_{i,j}$
3:	Find $\mathbb{M}_{d_{i,j} \times P}$ from $\mathbb{L}$, *s.t.*, $\mathbb{M}_{l,m} < \varepsilon^{l,m}_{i,j}, \forall l, \forall m$
4:	**If** $\mathbb{M} \neq \emptyset$

5:	Find $\mathcal{R} = \arg\min_l$ (max of each row in $\mathbb{M}$)
6:	$\mathbf{F}^*_{i,j}$ = Row vector in $\mathbb{C}^a_{i,j}$ corresponding to $\mathcal{R}$
7:	**Else** $\mathbf{F}^*_{i,j} = \emptyset$
8:	**End If**

TABLE V: *(Inter-network Cooperation) Traffic Distribution of $\mathcal{B}_{i,j}$ if $\mathcal{L}_{i,j} < \vartheta_{i,j}, \forall i, \forall j$*

1:	Initialize $s_{i,j}, p_{i,j}, \mathcal{A}_{i,j}, \mathcal{S}_{i,j}, \mathcal{P}_{i,j}, \Psi_{i,j}, \mathbb{D}_{i,j}, \mathbb{D}^{L,a}_{i,j}$
2:	**If** $s_{i,j} = 1$, $\mathcal{L}_{i,j} < \vartheta_{i,j}$ and $\mathbb{D}^{L,a}_{i,j} \neq \emptyset$
3:	**If** $\sum_{k=1}^{\lvert\mathbb{D}^{L,a}_{i,j}\rvert} \left(\varepsilon^{(k)}_{i,j} - \mathcal{L}^{(k)}_{i,j}\right) \geq \mathcal{L}_{i,j}$, where $\mathcal{B}^{(k)}_{i,j} \in \mathbb{D}^{L,a}_{i,j}$
4:	Distribute $\mathcal{L}_{i,j}$ to $\mathcal{B}^{(k)}_{i,j} \in \mathbb{D}^{L,a}_{i,j}, \forall k = 1, 2, ..., \lvert\mathbb{D}^{L,a}_{i,j}\rvert$
5:	Set $\mathcal{L}_{i,j}, s_{i,j}, p_{i,j} = 0$; update $tf(\mathbb{D}^{L,a}_{i,j}), \mathcal{S}_{i,j}, \mathcal{P}_{i,j}$
6:	**End If**
7:	**End If**

TABLE VI: *(Inter-network Cooperation) Traffic Distribution of $\mathcal{B}_{i,j}$ if $\mathcal{L}_{i,j} \geq \omega_{i,j}, \forall i, \forall j$*

1:	Initialize $s_{i,j}, p_{i,j}, \mathcal{A}_{i,j}, \mathcal{S}_{i,j}, \mathcal{P}_{i,j}, \Psi_{i,j}, \mathbb{D}_{i,j}, \mathbb{D}^{L,a}_{i,j}, \mathbb{D}^{L,s}_{i,j}, \mathbb{D}^{H,a}_{i,j}, \mathbb{D}^{H,s}_{i,j}, \mathbb{S}$
2:	**If** $s_{i,j} = 1$, $\mathcal{L}_{i,j} \geq \omega_{i,j}$ and $\mathbb{D}^{L,a}_{i,j} \neq \emptyset$
3:	**If** $\sum_{k=1}^{\lvert\mathbb{D}_{i,j}\rvert} \left(\varepsilon^{(k)}_{i,j} - \mathcal{L}^{(k)}_{i,j}\right) \geq \mathcal{L}_{i,j}$, where $\mathcal{B}^{(k)}_{i,j} \in \mathbb{D}_{i,j}$
4:	Distribute $\mathcal{L}_{i,j}$ to $\mathcal{B}^{(k)}_{i,j} \in \mathbb{D}_{i,j}$ according to $\mathbb{S}$
5:	Set $\mathcal{L}_{i,j}, s_{i,j}, p_{i,j} = 0$; update $tf(\mathbb{D}_{i,j}), \mathcal{S}_{i,j}, \mathcal{P}_{i,j}$
7:	**Elseif** $\sum_{k=1}^{\lvert\mathbb{D}_{i,j}\rvert} \left(\varepsilon^{(k)}_{i,j} - \mathcal{L}^{(k)}_{i,j}\right) \geq \left(\mathcal{L}_{i,j} - \omega_{i,j}\right)$, where $\mathcal{B}^{(k)}_{i,j} \in \mathbb{D}_{i,j}$
8:	Distribute $\left(\mathcal{L}_{i,j} - \omega_{i,j}\right)$ to $\mathcal{B}^{(k)}_{i,j} \in \mathbb{D}_{i,j}$ according to $\mathbb{S}$
9:	Set $\mathcal{L}_{i,j} = \omega_{i,j}$; and update $p_{i,j}, tf(\mathbb{D}_{i,j}), \mathcal{S}_{i,j}, \mathcal{P}_{i,j}$
10:	**End If**
11:	**End If**

TABLE VII: *Joint Cooperation among N E-UTRANs*

1:	Initialize $\mathcal{I}_{i,j}, \mathcal{A}_{i,j}, \mathcal{S}_{i,j}, \mathcal{X}_{i,j}, \mathcal{P}_{i,j}, \Psi_{i,j}, \mathbf{U}_{i,j}, \mathbf{V}_{i,j}, \mathbb{C}_{i,j}, \mathbb{C}^a_{i,j}, \mathbb{C}^s_{i,j}, \mathbb{D}_{i,j}, \mathbb{D}^{L,a}_{i,j}, \mathbb{D}^{L,s}_{i,j}, \mathbb{D}^{H,a}_{i,j}, \mathbb{D}^{H,s}_{i,j}$
2:	*Intra-network cooperation* in each of the E-UTRANs
3:	*Inter-network cooperation* among all the E-UTRANs

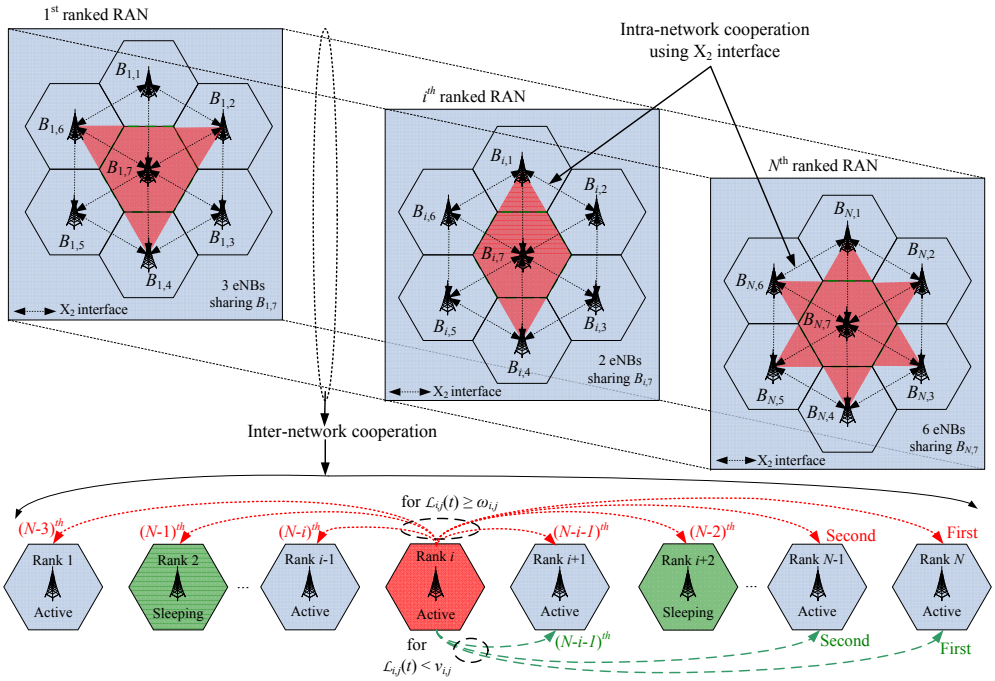

Fig. 1: System model of the proposed energy saving cooperative LTE cellular access networks.

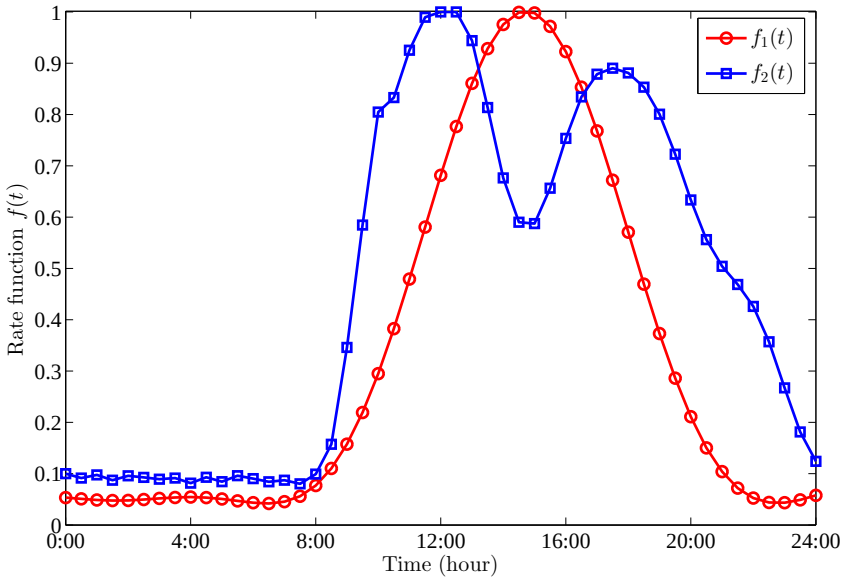

Fig. 2: Rate functions.

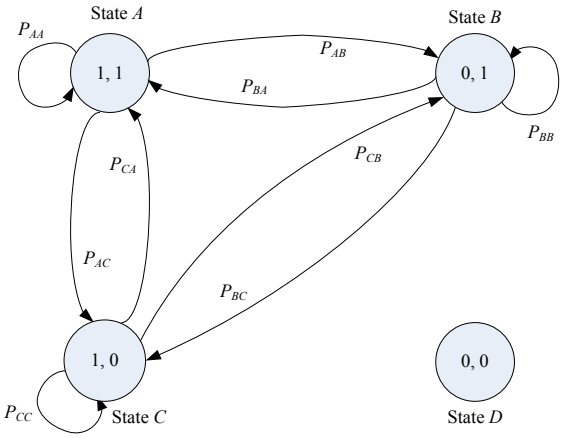

Fig. 3: Transition diagram for inter-network cooperation between two E-UTRANs.

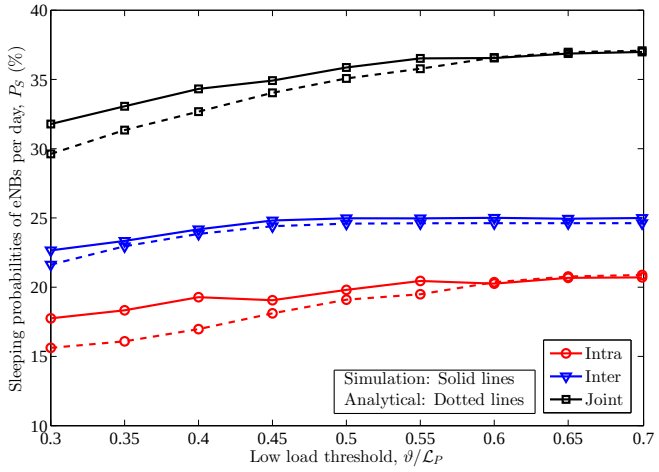

Fig. 4: Daily sleeping probabilities of eNBs with ϑ under S1.

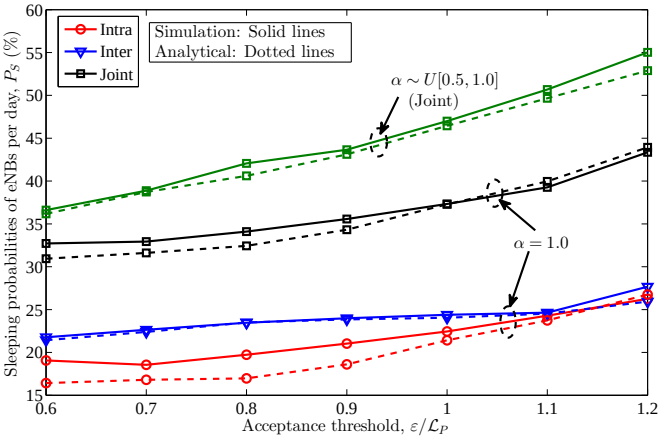

Fig. 5: Daily sleeping probabilities of eNBs with ε under S1.

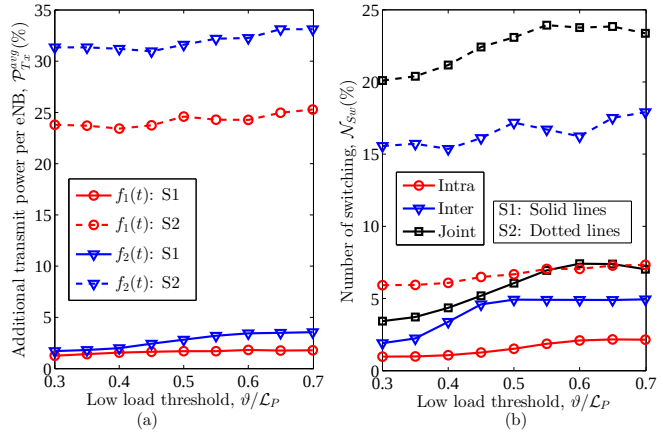

Fig. 6: Additional transmit power and number of switching per eNB.

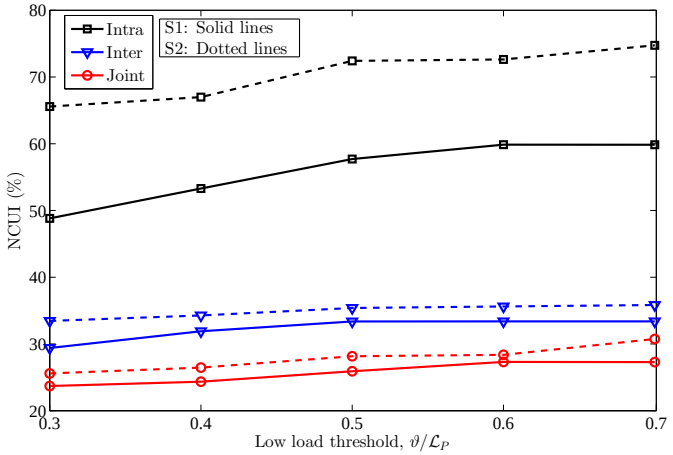

Fig. 7: Network capacity utilization improvement.

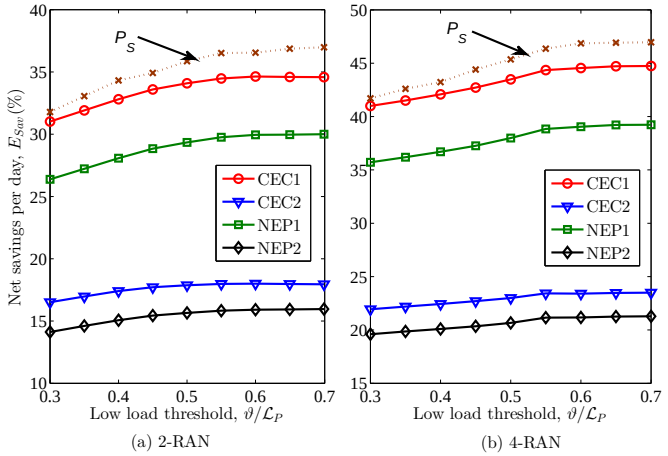

Fig. 8: Daily net energy savings from joint cooperation under S1.

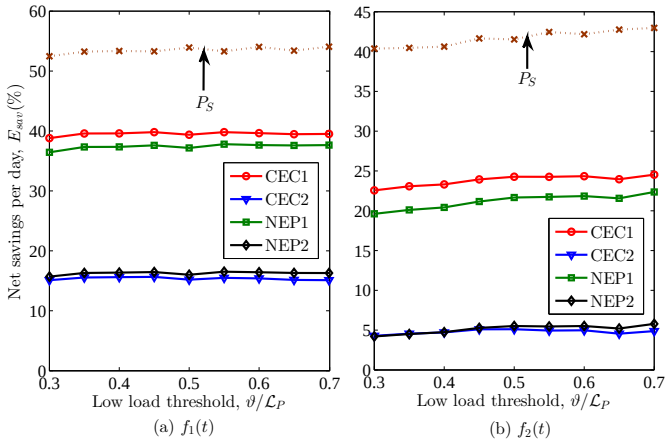

Fig. 9: Daily net energy savings from joint cooperation under S2.

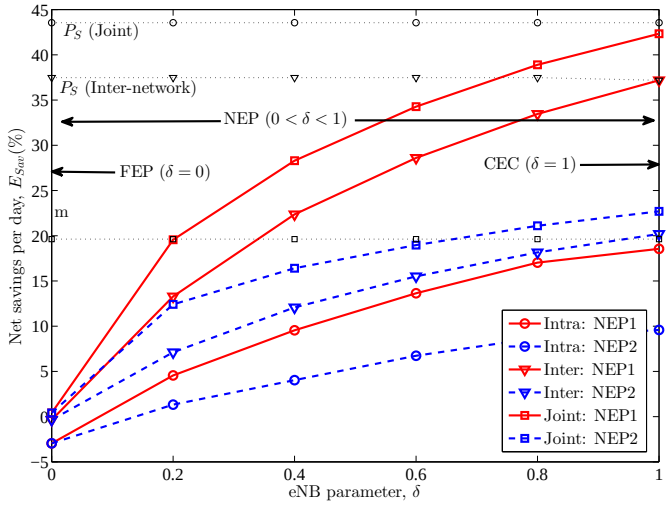

Fig. 10: Daily net energy savings with eNB parameter δ under S1.

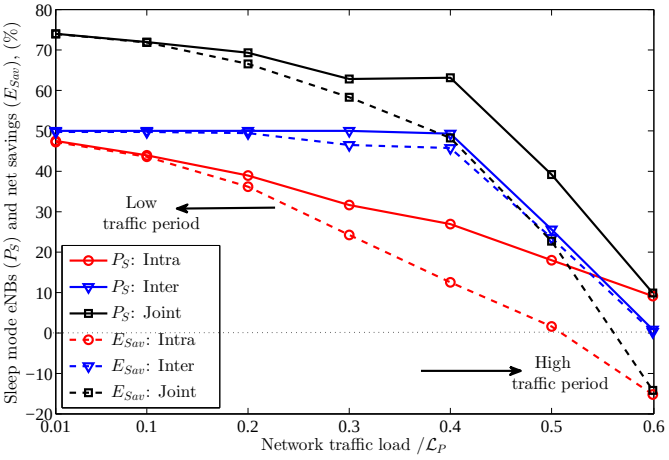

Fig. 11: Sleeping eNBs and net energy savings with time-homogeneous traffic generation.

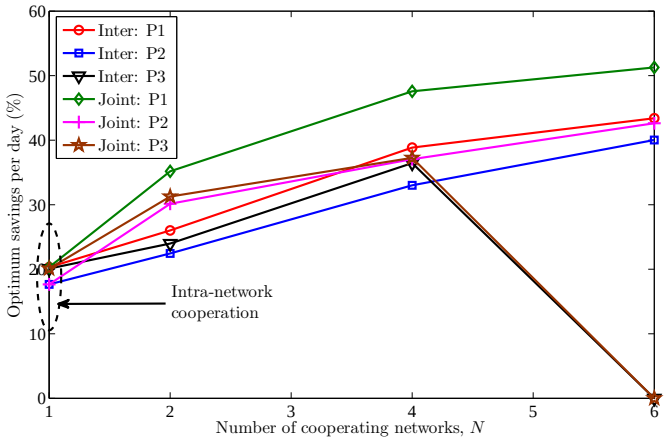

Fig. 12: Optimal daily energy savings under S1.

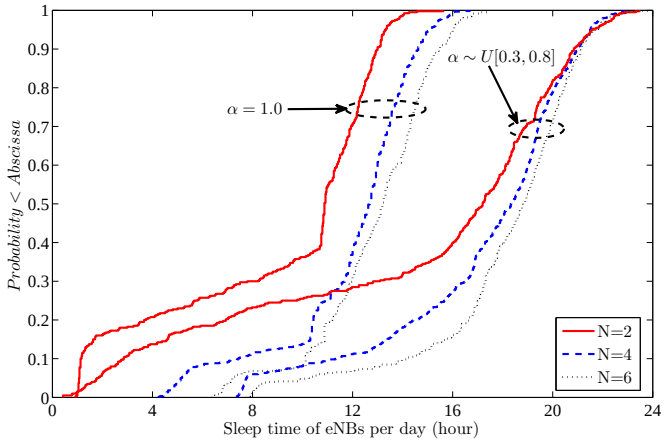

Fig. 13: CDF of daily sleep times of eNBs in joint cooperation with optimal settings under S1.

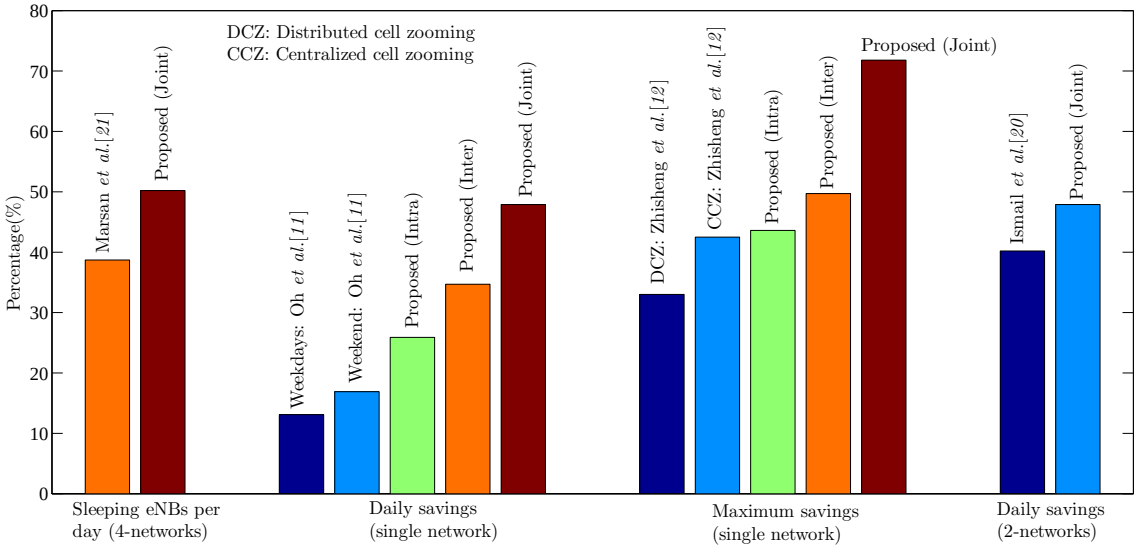

Fig. 14: Comparison chart.